

## Appendix A – Level densities in terms of measured fluorescence signals

We have established that the combinations of observed fluorescence intensities,

$$I^\perp \equiv I_{\text{Perp}}^{VH} + I_{\text{Par}}^{VH} + I_{\text{Perp}}^{HV} = h\nu_{e \rightarrow f} n_e V A_{e \rightarrow f} \mathcal{E}_{e \rightarrow f} \frac{d\Omega}{4\pi} \quad (\text{A1})$$

and

$$I^\parallel \equiv I_{\text{Perp}}^{VV} + I_{\text{Par}}^{VV} + I_{\text{Perp}}^{HH} = h\nu_{e \rightarrow f} n_e V A_{e \rightarrow f} \mathcal{E}_{e \rightarrow f} \frac{d\Omega}{4\pi} \quad (\text{A2})$$

(with units of Watts/emitted into solid angle  $d\Omega$ ) are proportional to the number density in the upper level,  $e$ , when the probe laser polarization is perpendicular to, or parallel to, the pump laser polarization, respectively. However, our goal is to study  $M$ - and  $J$ -changing collisions in the intermediate state  $i$ . Thus we must determine how the upper level density,  $n_e \equiv \sum_{M_e} n_{J_e, M_e}$ , relates to the directly excited intermediate level density,  $n_{J_i=1, M_i=0}$ , and to the densities of sublevels populated through  $M$ -changing collisions,  $n_{J_i=1, M_i=\pm 1}$ , and  $J$ -changing collisions,  $n_{J_i=3, 5, 7}$ , for the various pump/probe excitation schemes.

According to Eq. (16) of Jones *et al.* [1], the density in the upper level of a probe transition is given by

$$n_e = n_i \frac{P_{\text{probe}}^{e \leftarrow i}}{\left( \Gamma_e + k_{NG}^{Q,e} n_{NG} + k_{Li}^{Q,e} n_{Li} + P_{\text{probe}}^{e \rightarrow i} \right)}. \quad (\text{A3})$$

Here  $P_{\text{probe}}^{e \leftarrow i}$  and  $P_{\text{probe}}^{e \rightarrow i}$  are the probe laser excitation and stimulated emission rates, which are related to the Einstein  $B$  coefficient. Because we are considering excitation of individual  $M_i$  levels, it isn't necessary to include statistical weight factors, and the absorption and stimulated emission rates can be set equal:  $P_{\text{probe}}^{e \rightarrow i} = P_{\text{probe}}^{e \leftarrow i}$ .  $\Gamma_e \equiv \sum_{\ell} A_{e \rightarrow \ell}$ ,  $k_{NG}^{Q,e}$ , and  $k_{Li}^{Q,e}$  are the upper level total radiative rate, and the upper level total quenching rate coefficients due to collisions with noble gas and lithium atoms, respectively ( $n_{NG}$  and  $n_{Li}$  are the densities of the noble gas and lithium atom collision partners).

In the weak probe limit,  $P_{\text{probe}}^{e \rightarrow i} \ll \Gamma_e + k_{NG}^{Q,e} n_{NG} + k_{Li}^{Q,e} n_{Li}$ , Eq. (A3) reduces to Eq. (18) of Jones *et al.* [1]

$$n_e = \frac{P_{\text{probe}}^{e \leftarrow i}}{\left( \Gamma_e + k_{NG}^{Q,e} n_{NG} + k_{Li}^{Q,e} n_{Li} \right)} n_i. \quad (\text{A4})$$

The probe laser excitation rate  $P_{\text{probe}}^{e \leftarrow i}$  is given by [2, 3],

$$P_{\text{probe}}^{e \leftarrow i} = \int B_{e \leftarrow i}^I(\nu) I_{\text{Probe}}(\nu) d\nu = \frac{|\mu_{ei}|^2}{6\epsilon_0 \hbar^2 c} \int g(\nu - \nu_{e \leftarrow i}) I_{\text{Probe}}(\nu) d\nu. \quad (\text{A5})$$

Here the Einstein  $B$  coefficient is defined in terms of laser intensity, which is related to the more common  $B$  coefficient defined in terms of radiation density by  $B_{e \leftarrow i}^I(\nu) = B_{e \leftarrow i}^\rho(\nu) \frac{\rho(\nu)}{I(\nu)}$  – see

Eq. (9.44), page 283 of Corney [4],  $g(\nu - \nu_{e \leftarrow i})$  is the molecular absorption lineshape function for the  $e \leftarrow i$  transition (typically homogeneously broadened since the pump laser only excites one velocity group in level  $i$ ), and  $I_{\text{Probe}}(\nu) d\nu$  is the laser intensity in the frequency interval between  $\nu$  and  $\nu + d\nu$ . We don't include the intermediate level degeneracy factor  $(2J_i + 1)$  given in Eq. (9.46) of Corney, because we consider the contribution from pumping each individual  $M_i$  sublevel separately and sum over the  $M_i$  contributions at a later stage. The laser has very narrow bandwidth (which can be considered to be a delta function) and is tuned to line center of the probe transition. Therefore we can take  $I_{\text{Probe}}(\nu) = I_{\text{Probe}} \delta(\nu - \nu_{e \leftarrow i})$ , and Eq. (A5) reduces to

$$P_{\text{probe}}^{e \leftarrow i} = B_{e \leftarrow i}^I I_{\text{Probe}} = \frac{|\mu_{ei}|^2}{6\epsilon_0 \hbar^2 c} g(0) I_{\text{Probe}}. \quad (\text{A6})$$

where  $g(0)$  is the lineshape function evaluated at line center (with units  $\text{frequency}^{-1}$ ) and  $I_{\text{Probe}}$  is the total probe laser intensity ( $\text{W/m}^2$ ).

The electric dipole matrix element can be written as

$$\bar{\mu}_{ei} = \langle \Phi_e^{\text{el}} \chi_e^{\text{vib}} \varphi_e^{\text{rot}} | \hat{\mu} | \Phi_i^{\text{el}} \chi_i^{\text{vib}} \varphi_i^{\text{rot}} \rangle, \quad (\text{A7})$$

where  $\Phi_j^{\text{el}}$ ,  $\chi_j^{\text{vib}}$ , and  $\varphi_j^{\text{rot}}$  represent electronic, vibrational and rotational wave functions, respectively, and the integration is over all nuclear and electronic coordinates. The molecular electric dipole operator can be written as  $\hat{\mu} = \sum_n Z_n e \bar{R}_n - \sum_j e \vec{r}_j$  (here  $e$  is the charge on the electron and  $Z_n$  is the atomic number of nucleus  $n$ ), where the first term is a sum over nuclear coordinates while the second is a sum over electron coordinates. For electronic transitions (as studied here) only the second term contributes because the electronic wave functions are orthogonal. Consequently, we can rewrite (A7) as

$$\bar{\mu}_{ei} = -e \sum_{M_e} \langle \alpha_e, v_e, J_e, M_e | \sum_j \vec{r}_j | \alpha_i, v_i, J_i, M_i \rangle, \quad (\text{A8})$$

where  $\alpha_e$  and  $\alpha_i$  represent all other quantum numbers necessary to describe the upper (excited) and lower (intermediate) states. We sum over all possible excited state sublevels.

The probe laser intensity is related to probe laser electric field vector  $\hat{\epsilon}_{L2}E_{L2}$  by [Corney Eqs. (2.47) and (9.45)]

$$I_{\text{Probe}} = \frac{c\mathcal{E}_0}{8\pi} \left| \hat{\epsilon}_{L2}^* E_{L2} \cdot \hat{\epsilon}_{L2} E_{L2} \right|^2, \quad (\text{A9})$$

where  $\hat{\epsilon}_{L2}$  is a unit vector describing the probe laser polarization. To take into account the probe laser polarization in absorption we must first take the dot product of the electric field vector with the dipole matrix element before these terms are squared in Eq. (A6). Combining this with (A7) through (A9) and defining  $\bar{r} \equiv \sum_j \bar{r}_j$  (note that for alkali molecules we are generally only concerned about transitions involving a single electron), we find that

$$P_{\text{probe}}^{e \leftarrow i} = B_{e \leftarrow i}^I I_{\text{Probe}} = \frac{e^2 \sum_{M_e} \left| \langle \alpha_e, v_e, J_e, M_e | \hat{\epsilon}_{L2} \cdot \bar{r} | \alpha_i, v_i, J_i, M_i \rangle \right|^2}{48\pi\hbar^2} g(0) |E_{L2}|^2. \quad (\text{A10})$$

Plugging (A4) and (A10) into (A1) and (A2), and noting that we must also sum over all intermediate levels  $M_i$  that may contribute to the signal, we find:

$$\begin{aligned} I^\perp &\equiv I_{\text{Perp}}^{VH} + I_{\text{Par}}^{VH} + I_{\text{Perp}}^{HV} \\ &= \frac{h\nu_{e \rightarrow f} V A_{e \rightarrow f} \epsilon_{e \rightarrow f} e^2}{48\pi\hbar^2} \frac{g(0)}{(\Gamma_e + k_{NG}^{Q,e} n_{NG} + k_{Li}^{Q,e} n_{Li})} \frac{d\Omega}{4\pi} |E_{L2}|^2 \sum_{M_i, M_e} n_{v_i, J_i, M_i} \left| \langle \alpha_e, v_e, J_e, M_e | \hat{i} \cdot \bar{r} | \alpha_i, v_i, J_i, M_i \rangle \right|^2 \end{aligned} \quad (\text{A11})$$

and

$$\begin{aligned} I^\parallel &\equiv I_{\text{Perp}}^{VV} + I_{\text{Par}}^{VV} + I_{\text{Perp}}^{HH} \\ &= \frac{h\nu_{e \rightarrow f} V A_{e \rightarrow f} \epsilon_{e \rightarrow f} e^2}{48\pi\hbar^2} \frac{g(0)}{(\Gamma_e + k_{NG}^{Q,e} n_{NG} + k_{Li}^{Q,e} n_{Li})} \frac{d\Omega}{4\pi} |E_{L2}|^2 \sum_{M_i, M_e} n_{v_i, J_i, M_i} \left| \langle \alpha_e, v_e, J_e, M_e | \hat{k} \cdot \bar{r} | \alpha_i, v_i, J_i, M_i \rangle \right|^2, \end{aligned} \quad (\text{A12})$$

where we have used the fact that  $\hat{\epsilon}_{L2} \equiv \hat{i}$  when pump and probe laser polarization vectors are perpendicular, but  $\hat{\epsilon}_{L2} \equiv \hat{k}$  when they are parallel.

In our experiments using  $G^1\Pi_g(v_e=5, J_e) \leftarrow A^1\Sigma_u^+(v_i=5, J_i)$  probe transitions, we probe on Q-line transitions (i.e.,  $J_e = J_i$ ) and observe fluorescence on Q-line transitions (i.e.,  $J_f = J_e$ ). Eq. (11) in Chapter 3, Sec. 9 of Condon and Shortley [5] states that quantum mechanical matrix elements of a vector operator such as  $\vec{r}$ , with respect to angular momentum wave functions, obey the following relations when  $J_e = J_i$ :

$$\begin{aligned} \langle \alpha_e, v_e, J_e, M_e | \vec{r} | \alpha_i, v_i, J_i = J_e, M_i = M_e \pm 1 \rangle &= (\alpha_e, v_e, J_e | r | \alpha_i, v_i, J_i = J_e) \frac{1}{2} \sqrt{(J_e \mp M_e)(J_e \pm M_e + 1)} (\hat{i} \pm \hat{j}) \\ &= (\alpha_e, v_e, J_e = J_i | r | \alpha_i, v_i, J_i) \frac{1}{2} \sqrt{(J_i \mp M_i + 1)(J_i \pm M_i)} (\hat{i} \pm \hat{j}) \end{aligned} \quad (\text{A13})$$

and

$$\begin{aligned} \langle \alpha_e, v_e, J_e, M_e | \vec{r} | \alpha_i, v_i, J_i = J_e, M_i = M_e \rangle &= (\alpha_e, v_e, J_e | r | \alpha_i, v_i, J_i = J_e) M_e \hat{k} \\ &= (\alpha_e, v_e, J_e = J_i | r | \alpha_i, v_i, J_i) M_i \hat{k}, \end{aligned} \quad (\text{A14})$$

where  $(\alpha_e, v_e, J_e | r | \alpha_i, v_i, J_i)$  is called the ‘‘reduced matrix element’’ (which is independent of the  $M$  values). Thus (A11) and (A12) reduce to

$$\begin{aligned} [I^\perp]_{\text{Probe } J_i \rightarrow J_e = J_i} &\equiv [I_{\text{Perp}}^{VH} + I_{\text{Par}}^{VH} + I_{\text{Perp}}^{HV}]_{\text{Probe } J_i \rightarrow J_e = J_i} \\ &= \frac{h\nu_{e \rightarrow f} V A_{e \rightarrow f} \mathcal{E}_{e \rightarrow f} e^2}{48\pi\hbar^2} \frac{g(0)}{(\Gamma_e + k_{\text{NG}}^{Q,e} n_{\text{NG}} + k_{\text{Li}}^{Q,e} n_{\text{Li}})} \frac{d\Omega}{4\pi} |E_{L2}|^2 \left| (\alpha_e, v_e, J_e = J_i | r | \alpha_i, v_i, J_i) \right|^2 \\ &\times \sum_{M_i, M_e} n_{v_i, J_i, M_i} \frac{(J_i \mp M_i + 1)(J_i \pm M_i)}{4} \delta_{M_e, M_i \mp 1} \end{aligned} \quad (\text{A15})$$

and

$$\begin{aligned}
\left[ I^{\parallel} \right]_{\text{Probe } J_i \rightarrow J_e = J_i} &\equiv \left[ I_{\text{Perp}}^{VV} + I_{\text{Par}}^{VV} + I_{\text{Perp}}^{HH} \right]_{\text{Probe } J_i \rightarrow J_e = J_i} \\
&= \frac{h\nu_{e \rightarrow f} V A_{e \rightarrow f} \epsilon_{e \rightarrow f} e^2}{48\pi \hbar^2} \frac{g(0)}{\left( \Gamma_e + k_{NG}^{Q,e} n_{NG} + k_{Li}^{Q,e} n_{Li} \right)} \frac{d\Omega}{4\pi} |E_{L2}|^2 \left| \langle \alpha_e, v_e, J_e = J_i | r | \alpha_i, v_i, J_i \rangle \right|^2 \quad (\text{A16}) \\
&\times \sum_{M_i, M_e} n_{v_i, J_i, M_i} M_i^2 \delta_{M_e, M_i}.
\end{aligned}$$

However, in our experiments using  $F^1\Sigma_g^+(v_e = 12, J_e = 0) \leftarrow A^1\Sigma_u^+(v_i = 5, J_i = 1)$  probe transitions, we probe on P-line transitions (i.e.,  $J_e = J_i - 1$ ) and observe fluorescence on P-line transitions (i.e.,  $J_f = J_e + 1$ ). In this case, Eq. (11) in Chapter 3, Sec. 9 of Condon and Shortley [5] states that quantum mechanical matrix elements of a vector operator such as  $\vec{r}$ , with respect to angular momentum wave functions, obey the following relations when  $J_e = J_i - 1$ :

$$\begin{aligned}
&\langle \alpha_e, v_e, J_e, M_e | \vec{r} | \alpha_i, v_i, J_i = J_e + 1, M_i = M_e \pm 1 \rangle \\
&= \mp \langle \alpha_e, v_e, J_e | r | \alpha_i, v_i, J_i = J_e + 1 \rangle \frac{1}{2} \sqrt{(J_e \pm M_e + 1)(J_e \pm M_e + 2)} (\hat{i} \pm \hat{j}) \quad (\text{A17}) \\
&= \mp \langle \alpha_e, v_e, J_e = J_i - 1 | r | \alpha_i, v_i, J_i \rangle \frac{1}{2} \sqrt{(J_i \pm M_i - 1)(J_i \pm M_i)} (\hat{i} \pm \hat{j})
\end{aligned}$$

and

$$\begin{aligned}
\langle \alpha_e, v_e, J_e, M_e | \vec{r} | \alpha_i, v_i, J_i = J_e + 1, M_i = M_e \rangle &= \langle \alpha_e, v_e, J_e | r | \alpha_i, v_i, J_i = J_e + 1 \rangle \sqrt{(J_e + 1)^2 - M_e^2} \hat{k} \\
&= \langle \alpha_e, v_e, J_e = J_i - 1 | r | \alpha_i, v_i, J_i \rangle \sqrt{J_i^2 - M_i^2} \hat{k}. \quad (\text{A18})
\end{aligned}$$

Therefore, in this case, (A11) and (A12) reduce to

$$\begin{aligned}
\left[ I^\perp \right]_{\text{Probe } J_i \rightarrow J_e = J_i - 1} &\equiv \left[ I_{\text{Perp}}^{VH} + I_{\text{Par}}^{VH} + I_{\text{Perp}}^{HV} \right]_{\text{Probe } J_i \rightarrow J_e = J_i - 1} \\
&= \frac{h\nu_{e \rightarrow f} V A_{e \rightarrow f} \mathcal{E}_{e \rightarrow f} e^2}{48\pi\hbar^2} \frac{g(0)}{(\Gamma_e + k_{NG}^{Q,e} n_{NG} + k_{Li}^{Q,e} n_{Li})} \frac{d\Omega}{4\pi} |E_{L2}|^2 \left| (\alpha_e, v_e, J_e = J_i - 1 | r | \alpha_i, v_i, J_i) \right|^2 \\
&\times \sum_{M_i, M_e} n_{v_i, J_i, M_i} \frac{(J_i \pm M_i - 1)(J_i \pm M_i)}{4} \delta_{M_e, M_i \mp 1}
\end{aligned} \tag{A19}$$

and

$$\begin{aligned}
\left[ I^\parallel \right]_{\text{Probe } J_i \rightarrow J_e = J_i - 1} &\equiv \left[ I_{\text{Perp}}^{VV} + I_{\text{Par}}^{VV} + I_{\text{Perp}}^{HH} \right]_{\text{Probe } J_i \rightarrow J_e = J_i - 1} \\
&= \frac{h\nu_{e \rightarrow f} V A_{e \rightarrow f} \mathcal{E}_{e \rightarrow f} e^2}{48\pi\hbar^2} \frac{g(0)}{(\Gamma_e + k_{NG}^{Q,e} n_{NG} + k_{Li}^{Q,e} n_{Li})} \frac{d\Omega}{4\pi} |E_{L2}|^2 \left| (\alpha_e, v_e, J_e = J_i - 1 | r | \alpha_i, v_i, J_i) \right|^2 \\
&\times \sum_{M_i, M_e} n_{v_i, J_i, M_i} (J_i^2 - M_i^2) \delta_{M_e, M_i}.
\end{aligned} \tag{A20}$$

**i)  $M$ -changing collisions – Probe  $G^1\Pi_g(v_e = 5, J_e = J_i = 1) \leftarrow A^1\Sigma_u^+(v_i = 5, J_i = 1)$**

For  $M$ -changing collisions studied using  $G^1\Pi_g(v_e = 5, J_e = J_i = 1) \leftarrow A^1\Sigma_u^+(v_i = 5, J_i = 1)$  probe transitions, we can evaluate the sums in Eqs. (A15) and (A16)

$$\sum_{M_i, M_e} n_{v_i, J_i, M_i} \frac{(J_i \mp M_i + 1)(J_i \pm M_i)}{4} \delta_{M_e, M_i \mp 1} = \sum_{M_i, M_e} n_{v_i, J_i = 1, M_i} \frac{(1 \mp M_i + 1)(1 \pm M_i)}{4} \delta_{M_e, M_i \mp 1} \tag{A21}$$

$$= \frac{n_{v_i, J_i = 1, M_i = -1}}{2} + \frac{2n_{v_i, J_i = 1, M_i = 0}}{2} + \frac{n_{v_i, J_i = 1, M_i = +1}}{2}$$

and

$$\sum_{M_i, M_e} n_{v_i, J_i, M_i} M_i^2 \delta_{M_e, M_i} = n_{v_i, J_i = 1, M_i = -1} + n_{v_i, J_i = 1, M_i = +1} \tag{A22}$$

which leads directly to the proportionalities

$$I^\perp \propto \frac{(n_{J_i=1, M_i=-1} + 2n_{J_i=1, M_i=0} + n_{J_i=1, M_i=+1})}{2} e^2 (E_{L2})^2 |(\alpha_e, v_e, J_e = 1 | \vec{r} | \alpha_i, v_i, J_i = 1)|^2 \quad (\text{A23})$$

and

$$I^\parallel \propto (n_{J_i=1, M_i=-1} + n_{J_i=1, M_i=+1}) e^2 (E_{L2})^2 |(\alpha_e, v_e, J_e = 1 | \vec{r} | \alpha_i, v_i, J_i = 1)|^2 \quad (\text{A24})$$

in the weak probe limit. These are Eqs. (8) and (9) of the main text. In our studies of  $M$ -changing collisions using the  $G^1\Pi_g(v_e = 5, J_e = J_i = 1) \leftarrow A^1\Sigma_u^+(v_i = 5, J_i = 1)$  probe transitions, the intermediate state is always  $A^1\Sigma_u^+(v_i = 5, J_i = 1)$ , the upper (excited) level of the probe transition is always  $G^1\Pi_g(v_e = 5, J_e = J_i = 1)$ , and the lower (final) level of the fluorescence transition is always  $A^1\Sigma_u^+(v_f = 6, J_f = J_e = 1)$ . The detection volume and detection solid angle also remain the same. Thus the factor

$$\frac{h\nu_{e \rightarrow f} V A_{e \rightarrow f} \mathcal{E}_{e \rightarrow f} e^2}{48\pi\hbar^2} \frac{g(0)}{(\Gamma_e + k_{NG}^{Q,e} n_{NG} + k_{Li}^{Q,e} n_{Li})} \frac{d\Omega}{4\pi} |(\alpha_e v_e J_e | r | \alpha_i v_i J_i)|^2 \text{ can be taken to be constant.}$$

Taking a ratio of fluorescence intensities, as in Eqs. (10) and (11) of the main text, we see that the proportionality factors cancel completely (we maintain the probe laser intensity constant over a series of measurements). Thus we arrive at

$$\begin{aligned} \left[ \frac{2I^\parallel}{2I^\perp - I^\parallel} \right]_{\text{Probe } J_i=1 \rightarrow G^1\Pi_g} &= \left[ \frac{2(I_{\text{Perp}}^{VV} + I_{\text{Par}}^{VV} + I_{\text{Perp}}^{HH})}{2(I_{\text{Perp}}^{VH} + I_{\text{Par}}^{VH} + I_{\text{Perp}}^{HV}) - (I_{\text{Perp}}^{VV} + I_{\text{Par}}^{VV} + I_{\text{Perp}}^{HH})} \right]_{\text{Probe } J_i=1 \rightarrow G^1\Pi_g} \\ &= \frac{(n_{J_i=1, M_i=-1} + n_{J_i=1, M_i=+1})}{n_{J_i=1, M_i=0}} \end{aligned} \quad (\text{A25})$$

and

$$\begin{aligned} R_{J_i=1(G^1\Pi_g)} &\equiv \left[ \frac{I^\parallel}{2I^\perp - I^\parallel} \right]_{\text{Probe } J_i=1 \rightarrow G^1\Pi_g} \\ &= \left[ \frac{(I_{\text{Perp}}^{VV} + I_{\text{Par}}^{VV} + I_{\text{Perp}}^{HH})}{2(I_{\text{Perp}}^{VH} + I_{\text{Par}}^{VH} + I_{\text{Perp}}^{HV}) - (I_{\text{Perp}}^{VV} + I_{\text{Par}}^{VV} + I_{\text{Perp}}^{HH})} \right]_{\text{Probe } J_i=1 \rightarrow G^1\Pi_g} = \frac{n_{J_i=1, M_i=\pm 1}}{n_{J_i=1, M_i=0}}, \end{aligned} \quad (\text{A26})$$

which are Eqs. (10) and (11). These equations describe the ratio of densities of collisionally populated and directly populated  $M$  levels of the intermediate state  $J_i = 1$ , in terms of ratios of measured fluorescence intensities.

**ii)  $M$ -changing collisions – Probe  $F^1\Sigma_g^+(v_e = 12, J_e = 0) \leftarrow A^1\Sigma_u^+(v_i = 5, J_i = 1)$**

For  $M$ -changing collisions studied using  $F^1\Sigma_g^+(v_e = 12, J_e = 0) \leftarrow A^1\Sigma_u^+(v_i = 5, J_i = 1)$  probe transitions, we can evaluate the sums in Eqs. (A19) and (A20)

$$\begin{aligned} \sum_{M_i, M_e} n_{v_i, J_i, M_i} \frac{(J_i \pm M_i - 1)(J_i \pm M_i)}{4} \delta_{M_e, M_i \mp 1} &= \sum_{M_i, M_e} n_{v_i, J_i=1, M_i} \frac{(1 \pm M_i - 1)(1 \pm M_i)}{4} \delta_{M_e, M_i \mp 1} \\ &= \frac{n_{v_i, J_i=1, M_i=-1}}{2} + \frac{n_{v_i, J_i=1, M_i=+1}}{2} \end{aligned} \quad (\text{A27})$$

and

$$\sum_{M_i, M_e} n_{v_i, J_i, M_i} (J_i^2 - M_i^2) \delta_{M_e, M_i} = \sum_{M_i, M_e} n_{v_i, J_i=1, M_i} (1^2 - M_i^2) \delta_{M_e, M_i} = n_{v_i, J_i=1, M_i=0}. \quad (\text{A28})$$

In our studies of  $M$ -changing collisions using the  $F^1\Sigma_g^+(v_e = 12, J_e = 0) \leftarrow A^1\Sigma_u^+(v_i = 5, J_i = 1)$  probe transitions, the intermediate state is always  $A^1\Sigma_u^+(v_i = 5, J_i = 1)$ , the upper (excited) level of the probe transition is always  $F^1\Sigma_g^+(v_e = 12, J_e = 0)$ , and the lower (final) level of the fluorescence transition is always  $A^1\Sigma_u^+(v_f = 6, J_f = J_e + 1 = 1)$ . The detection volume and detection solid angle also remain the same. Thus the factor

$\frac{h\nu_{e \rightarrow f} V A_{e \rightarrow f} \epsilon_{e \rightarrow f} e^2}{48\pi\hbar^2} \frac{g(0)}{(\Gamma_e + k_{NG}^{Q,e} n_{NG} + k_{Li}^{Q,e} n_{Li})} \frac{d\Omega}{4\pi} |(\alpha_e v_e J_e | r | \alpha_i v_i J_i)|^2$  can again be taken to be constant.

Plugging the sums determined in (A27) and (A28) into the intensity expressions (A19) and (A20) and taking a ratio, we see that the proportionality factors again cancel completely and we arrive at

$$\begin{aligned}
R_{J_i=1(F^1\Sigma_g^+)} &= \left[ \frac{I^\perp}{I^\parallel} \right]_{\text{Probe } J_i=1 \rightarrow F^1\Sigma_g^+} = \left[ \frac{I_{\text{Perp}}^{VH} + I_{\text{Par}}^{VH} + I_{\text{Perp}}^{HV}}{I_{\text{Perp}}^{VV} + I_{\text{Par}}^{VV} + I_{\text{Perp}}^{HH}} \right]_{\text{Probe } J_i=1 \rightarrow F^1\Sigma_g^+} \\
&= \frac{n_{v_i, J_i=1, m_i=-1} + n_{v_i, J_i=1, m_i=-1}}{2n_{v_i, J_i=1, m_i=0}} = \frac{n_{v_i, J_i=1, m_i=\pm 1}}{n_{v_i, J_i=1, m_i=0}},
\end{aligned} \tag{A29}$$

in the weak probe limit. This is Eq. (12). Again note that  $n_{J_i=1, M_i=\pm 1}$  represents the population in either the  $M_i = -1$  or the  $M_i = +1$  sublevel (not the sum).

### iii) $J$ -changing collisions

In our studies of  $J$ -changing collisions, the situation is slightly more complicated because the intermediate and excited levels involve different values of  $J_i$  and  $J_e$  for different probe transitions. We still probe on Q-line transitions (i.e.,  $J_e = J_i$ ) and observe fluorescence on Q-line transitions (i.e.,  $J_f = J_e$ ). Therefore, we evaluate matrix elements using (A13) and (A14). However, since  $J_i \neq 1$  and  $J_e \neq 1$  for all probe transitions, it is not obvious that proportionality factors relating level densities to measured intensities will still cancel. In this case, we consider the specific combination

$$\begin{aligned}
2I^\perp + I^\parallel &= \frac{h\nu_{e \rightarrow f} V A_{e \rightarrow f} \mathcal{E}_{e \rightarrow f} e^2}{48\pi\hbar^2} \frac{g(0)}{(\Gamma_e + k_{NG}^{Q,e} n_{NG} + k_{Li}^{Q,e} n_{Li})} \frac{d\Omega}{4\pi} |E_{L2}|^2 |(\alpha_e, v_e, J_e = J_i | r | \alpha_i, v_i, J_i)|^2 \\
&\times \sum_{M_i, M_e} n_{v_i, J_i, M_i} \left[ M_i^2 \delta_{M_e, M_i} + \frac{(J_i \mp M_i + 1)(J_i \pm M_i)}{2} \delta_{M_e, M_i \mp 1} \right] \\
&= \frac{h\nu_{e \rightarrow f} V A_{e \rightarrow f} \mathcal{E}_{e \rightarrow f} e^2}{48\pi\hbar^2} \frac{g(0)}{(\Gamma_e + k_{NG}^{Q,e} n_{NG} + k_{Li}^{Q,e} n_{Li})} \frac{d\Omega}{4\pi} |E_{L2}|^2 |(\alpha_e, v_e, J_e = J_i | r | \alpha_i, v_i, J_i)|^2 \\
&\times \sum_{M_i, M_e} n_{v_i, J_i, M_i} \left[ M_i^2 \delta_{M_e, M_i} + \frac{(J_i - M_i + 1)(J_i + M_i)}{2} \delta_{M_e, M_i - 1} + \frac{(J_i + M_i + 1)(J_i - M_i)}{2} \delta_{M_e, M_i + 1} \right].
\end{aligned} \tag{A30}$$

The delta functions eliminate the sums over  $M_e$  and we obtain:

$$\begin{aligned}
2I^\perp + I^\parallel &= \frac{h\nu_{e \rightarrow f} V A_{e \rightarrow f} \epsilon_{e \rightarrow f} e^2}{48\pi\hbar^2} \frac{g(0)}{(\Gamma_e + k_{NG}^{Q,e} n_{NG} + k_{Li}^{Q,e} n_{Li})} \frac{d\Omega}{4\pi} |E_{L2}|^2 \left| \langle \alpha_e, v_e, J_e = J_i | r | \alpha_i, v_i, J_i \rangle \right|^2 \\
&\times \sum_{M_i=-J_i}^{J_i} n_{v_i, J_i, M_i} \left[ M_i^2 + \frac{J_i^2 - M_i^2 + J_i + M_i}{2} + \frac{J_i^2 - M_i^2 + J_i - M_i}{2} \right] \\
&= \frac{h\nu_{e \rightarrow f} V A_{e \rightarrow f} \epsilon_{e \rightarrow f} e^2}{48\pi\hbar^2} \frac{g(0)}{(\Gamma_e + k_{NG}^{Q,e} n_{NG} + k_{Li}^{Q,e} n_{Li})} \frac{d\Omega}{4\pi} |E_{L2}|^2 \left| \langle \alpha_e, v_e, J_e = J_i | r | \alpha_i, v_i, J_i \rangle \right|^2 J_i (J_i + 1) \sum_{M_i=-J_i}^{J_i} n_{v_i, J_i, M_i}.
\end{aligned} \tag{A31}$$

According to Eq. (2), chapter 3 of Kovacs [6], the Einstein  $A$  coefficient for a molecular transition from upper level  $e$  to lower level  $i$  is given by

$$\begin{aligned}
A_{e \rightarrow i} &= \frac{8\pi^2 \nu_{e \rightarrow i}^3 |\mu_{ei}|^2}{3\epsilon_0 c^3 \hbar (2J_e + 1)} = \frac{8\pi^2 \nu_{e \rightarrow i}^3 e^2 \sum_{M_e, M_i} \left| \langle \alpha_e, v_e, J_e, M_e | \vec{r} | \alpha_i, v_i, J_i, M_i \rangle \right|^2}{3\epsilon_0 c^3 \hbar (2J_e + 1)} \\
&= \frac{8\pi^2 \nu_{e \rightarrow i}^3 e^2 \sum_{M_i} \left| \langle \alpha_e, v_e, J_e, M_e | \vec{r} | \alpha_i, v_i, J_i, M_i \rangle \right|^2}{3\epsilon_0 c^3 \hbar},
\end{aligned} \tag{A32}$$

where in the last step we used the fact that each of the  $2J_e + 1$  upper state  $M_e$  levels must decay with the same rate [note: Eq. (A32) agrees with Bernath [3] Eq. (1.52), Corney [4] Eq. (4.23), and Herzberg [2] Eq. (I,47)]. For Q-line transitions ( $J_e = J_i$ ) we can again use (A13) and (A14) to write this as

$$\begin{aligned}
A_{e \rightarrow i} &= \frac{8\pi^2 \nu_{e \rightarrow i}^3 e^2}{3\epsilon_0 c^3 \hbar} \left[ \left| \langle \alpha_e, v_e, J_e, M_e | \bar{r} | \alpha_i, v_i, J_i = J_e, M_i = M_e - 1 \rangle \right|^2 \right. \\
&\quad \left. + \left| \langle \alpha_e, v_e, J_e, M_e | \bar{r} | \alpha_i, v_i, J_i = J_e, M_i = M_e \rangle \right|^2 + \left| \langle \alpha_e, v_e, J_e, M_e | \bar{r} | \alpha_i, v_i, J_i = J_e, M_i = M_e + 1 \rangle \right|^2 \right] \\
&= \frac{8\pi^2 \nu_{e \rightarrow i}^3 e^2}{3\epsilon_0 c^3 \hbar} \left| \langle \alpha_e, v_e, J_e | r | \alpha_i, v_i, J_i = J_e \rangle \right|^2 \left[ (J_e + M_e)(J_e - M_e + 1) \frac{(\hat{i} - \hat{j}) \cdot (\hat{i} + \hat{j})}{4} \right. \\
&\quad \left. + M_e^2 (\hat{k} \cdot \hat{k}) + (J_e - M_e)(J_e + M_e + 1) \frac{(\hat{i} + \hat{j}) \cdot (\hat{i} - \hat{j})}{4} \right] \\
&= \frac{8\pi^2 \nu_{e \rightarrow i}^3 e^2}{3\epsilon_0 c^3 \hbar} J_e (J_e + 1) \left| \langle \alpha_e, v_e, J_e | r | \alpha_i, v_i, J_i = J_e \rangle \right|^2.
\end{aligned} \tag{A33}$$

This establishes the relationship between the reduced matrix element and the Einstein  $A$  coefficient for Q-line transitions:

$$\left| \langle \alpha_e v_e J_e | r | \alpha_i v_i J_i = J_e \rangle \right|^2 = \frac{3\epsilon_0 c^3 \hbar}{8\pi^2 \nu_{e \rightarrow i}^3 e^2} \frac{A_{e \rightarrow i}}{J_e (J_e + 1)}. \tag{A34}$$

Finally, going back to (A32), we can now determine how the Einstein  $A$  coefficient varies with upper and lower level rotational quantum numbers. Using the Born-Oppenheimer approximation, the electronic, vibrational, and rotational motions can be taken to be mutually independent and we can separate the square of the matrix element as

$$|\mu_{ei}|^2 = e^2 S_{J_e, J_i} \left| \int \chi_e^{v*} \chi_i^v dR \int \Phi_e^{el*} \bar{r} \Phi_i^{el} d\tau_{el} \right|^2. \tag{A35}$$

where the rotational level dependence is contained in the Hönl-London factors,  $S_{J_e, J_i}$ . Inserting this into (A32) we find

$$A_{e \rightarrow i} = \frac{8\pi^2 \nu_{e \rightarrow i}^3 |\mu_{ei}|^2}{3\epsilon_0 c^3 \hbar (2J_e + 1)} = \frac{8\pi^2 \nu_{e \rightarrow i}^3 e^2}{3\epsilon_0 c^3 \hbar (2J_e + 1)} S_{J_e, J_i} \left| \int \chi_e^{v*} \chi_i^v dR \int \Phi_e^{el*} \bar{r} \Phi_i^{el} d\tau_{el} \right|^2. \tag{A36}$$

In our  $J$ -changing collision experiments, the probe and fluorescence channels both involve Q-line transitions between an upper  $^1\Pi$  state and a lower  $^1\Sigma$  state. The Hönl-London factor for such transitions is given by Eq. (IV,82) (page 208) of Herzberg [2]:

$$S_{J_e, J_i} = \frac{(J_e + \Lambda_e)(J_e + 1 - \Lambda_e)(2J_e + 1)}{4J_e(J_e + 1)} = \frac{(2J_e + 1)}{4}, \quad (\text{A37})$$

where  $\Lambda_e = 1$  and  $\Lambda_i = 0$  are the projections of electron orbital angular momentum onto the internuclear axis for the upper and lower levels, respectively. Plugging (A37) into (A36), we see that, to good approximation, the molecular Einstein  $A$  coefficients for Q-line transitions between the same electronic and vibrational levels are approximately independent of rotational quantum number. We also note that, according to Eq. (IV,82) (page 208) of Herzberg [2], the Hönl-London factors for P- and R-line transitions between an upper  ${}^1\Pi$  state and a lower  ${}^1\Sigma$  state are  $J_e/4$  and  $(J_e + 1)/4$ , respectively. Thus the sum of Einstein  $A$  coefficients for P- and R-line transitions is also independent of rotational quantum number to a good approximation.

In the  $J$ -changing collision studies, we measure the fluorescence intensities  $I_{\text{Perp}}^{VH}$ ,  $I_{\text{Par}}^{VH}$ ,  $I_{\text{Perp}}^{HV}$ ,  $I_{\text{Perp}}^{VV}$ ,  $I_{\text{Par}}^{VV}$ , and  $I_{\text{Perp}}^{HH}$  when probing either the directly excited ( $J'_i = 1$ ) or one of the collisional populated ( $J_i = 3, 5, \text{ or } 7$ ) levels and determine the quantities  $2I^\perp + I^\parallel$  using (A11), (A12), (A15), and (A16). We then calculate the ratio

$$\begin{aligned}
R_{J_i=3,5,7} &= \frac{\left[ 2I^\perp + I^\parallel \right]_{\text{Probe } J_i=3,5,7 \rightarrow G^1\Pi_g}}{\left[ 2I^\perp + I^\parallel \right]_{\text{Probe } J'_i=1 \rightarrow G^1\Pi_g}} = \frac{\left[ 2(I_{\text{Perp}}^{VH} + I_{\text{Par}}^{VH} + I_{\text{Perp}}^{HV}) + (I_{\text{Perp}}^{VV} + I_{\text{Par}}^{VV} + I_{\text{Perp}}^{HH}) \right]_{\text{Probe } J_i=3,5,7 \rightarrow G^1\Pi_g}}{\left[ 2(I_{\text{Perp}}^{VH} + I_{\text{Par}}^{VH} + I_{\text{Perp}}^{HV}) + (I_{\text{Perp}}^{VV} + I_{\text{Par}}^{VV} + I_{\text{Perp}}^{HH}) \right]_{\text{Probe } J'_i=1 \rightarrow G^1\Pi_g}} \\
&= \frac{\left[ \frac{h\nu_{e \rightarrow f} V A_{e \rightarrow f} \epsilon_{e \rightarrow f} e^2}{48\pi\hbar^2} \frac{g(0)}{(\Gamma_e + k_{NG}^{Q,e} n_{NG} + k_{Li}^{Q,e} n_{Li})} \frac{d\Omega}{4\pi} |E_{L2}|^2 \right. \\
&\quad \left. \times |(\alpha_e, v_e, J_e = J_i | r | \alpha_i, v_i, J_i = 3, 5, 7)|^2 J_i (J_i + 1) \sum_{M_i=-J_i}^{J_i} n_{v_i, J_i, M_i} \right]_{\text{Probe } J_i=3,5,7 \rightarrow G^1\Pi_g}}{\left[ \frac{h\nu_{e \rightarrow f} V A_{e \rightarrow f} \epsilon_{e \rightarrow f} e^2}{48\pi\hbar^2} \frac{g(0)}{(\Gamma_e + k_{NG}^{Q,e} n_{NG} + k_{Li}^{Q,e} n_{Li})} \frac{d\Omega}{4\pi} |E_{L2}|^2 \right. \\
&\quad \left. \times |(\alpha_e, v_e, J'_e = J'_i | r | \alpha_i, v_i, J'_i = 1)|^2 J'_i (J'_i + 1) \sum_{M'_i=-J'_i}^{J'_i} n_{v_i, J'_i, M'_i} \right]_{\text{Probe } J'_i=1 \rightarrow G^1\Pi_g}} \\
&= \frac{\left[ \frac{h\nu_{e \rightarrow f} V A_{e \rightarrow f} \epsilon_{e \rightarrow f} e^2}{48\pi\hbar^2} \frac{g(0)}{(\Gamma_e + k_{NG}^{Q,e} n_{NG} + k_{Li}^{Q,e} n_{Li})} \frac{d\Omega}{4\pi} |E_{L2}|^2 \frac{3\varepsilon_0 c^3 \hbar}{8\pi^2 \nu_{e \rightarrow i}^3 e^2} \frac{A_{e \rightarrow i}}{J_e (J_e + 1)} J_i (J_i + 1) \sum_{M_i=-J_i}^{J_i} n_{v_i, J_i, M_i} \right]_{\text{Probe } J_i=3,5,7 \rightarrow G^1\Pi_g}}{\left[ \frac{h\nu_{e \rightarrow f} V A_{e \rightarrow f} \epsilon_{e \rightarrow f} e^2}{48\pi\hbar^2} \frac{g(0)}{(\Gamma_e + k_{NG}^{Q,e} n_{NG} + k_{Li}^{Q,e} n_{Li})} \frac{d\Omega}{4\pi} |E_{L2}|^2 \frac{3\varepsilon_0 c^3 \hbar}{8\pi^2 \nu_{e \rightarrow i}^3 e^2} \frac{A_{e \rightarrow i}}{J'_e (J'_e + 1)} J'_i (J'_i + 1) \sum_{M'_i=-J'_i}^{J'_i} n_{v_i, J'_i, M'_i} \right]_{\text{Probe } J'_i=1 \rightarrow G^1\Pi_g}}
\end{aligned} \tag{A38}$$

where we used (A34) in the final step.

Negligible error is introduced if the Q-line probe laser transition frequencies in (A38) are taken to be identical since these transitions are part of the same vibrational band and differ by less than 0.01% for the transitions studied in the current work. The same is true for the Q-line fluorescence frequencies  $\nu_{e \rightarrow f}$  contained in the factor  $A_{e \rightarrow f}$ . The detection system efficiencies are also nearly identical at these closely spaced frequencies. Other factors, such as the probe laser power (and hence the laser electric field amplitude), detection volume, and detection solid angle are also unchanged over the course of a series of measurements. The factors  $\frac{J_i (J_i + 1)}{J_e (J_e + 1)} = 1$  and  $\frac{J'_i (J'_i + 1)}{J'_e (J'_e + 1)} = 1$  for Q-line probe transitions. And as can be inferred from Eqs.

(A36) and (A37) and the subsequent discussion, the total radiative rates are approximately equal for neighboring rotational levels of the same vibrational state. Finally, following Jones *et al.* [1], we assume that the quenching rates are approximately independent of rotational level (this approximation was theoretically verified to be approximately true by Price [7]). Introducing this information into Eq. (A38) we obtain

$$R_{J_i=3,5,7} = \frac{\left[ 2I^\perp + I^\parallel \right]_{\text{Probe } J_i=3,5,7 \rightarrow G^1\Pi_g}}{\left[ 2I^\perp + I^\parallel \right]_{\text{Probe } J'_i=1 \rightarrow G^1\Pi_g}} = \frac{\sum_{M_i=-J_i}^{J_i} n_{J_i=3,5,7,M_i}}{\sum_{M'_i=-J'_i}^{J'_i} n_{J'_i=1,M'_i}} = \frac{n_{J_i=3,5,7}}{n_{J'_i=1}}. \quad (\text{A35})$$

This is Eq. (13) in the main text.

## Appendix B - Error Analysis

The fitting functions used to determine the  $M$ -changing collisional rate coefficients are given by Eqs. (22) and (23) in the published manuscript:

$$R_{J_i=1(G^1\Pi_g)} \equiv \left[ \frac{I^\parallel}{2I^\perp - I^\parallel} \right]_{\text{Probe } J_i=1 \rightarrow G^1\Pi_g} \equiv \left[ \frac{(I_{\text{Perp}}^{VV} + I_{\text{Par}}^{VV} + I_{\text{Perp}}^{HH})}{2(I_{\text{Perp}}^{VH} + I_{\text{Par}}^{VH} + I_{\text{Perp}}^{HV}) - (I_{\text{Perp}}^{VV} + I_{\text{Par}}^{VV} + I_{\text{Perp}}^{HH})} \right]_{\text{Probe } J_i=1 \rightarrow G^1\Pi_g}$$

$$= \frac{\tilde{k}_{NG}^{J_i=1, M_i=0 \rightarrow \pm 1} n_{NG} + C_1}{1 + \tilde{k}_{NG}^Q n_{NG} + C_Q}, \quad (\text{B1})$$

and

$$R_{J_i=1(F^1\Sigma_g^+)} \equiv \left[ \frac{I^\perp}{I^\parallel} \right]_{\text{Probe } J_i=1 \rightarrow F^1\Sigma_g^+} \equiv \left[ \frac{I_{\text{Perp}}^{VH} + I_{\text{Par}}^{VH} + I_{\text{Perp}}^{HV}}{I_{\text{Perp}}^{VV} + I_{\text{Par}}^{VV} + I_{\text{Perp}}^{HH}} \right]_{\text{Probe } J_i=1 \rightarrow F^1\Sigma_g^+}$$

$$= \frac{\tilde{k}_{NG}^{J_i=1, M_i=0 \rightarrow \pm 1} n_{NG} + C_1}{1 + \tilde{k}_{NG}^Q n_{NG} + C_Q}, \quad (\text{B2})$$

for data obtained using the  $G^1\Pi_g (v_e = 5, J_e = J_i = 1) \leftarrow A^1\Sigma_u^+ (v_i = 5, J_i = 1)$  probe transition, and for data obtained using the  $F^1\Sigma_g^+ (v_e = 12, J_e = 0) \leftarrow A^1\Sigma_u^+ (v_i = 5, J_i = 1)$  probe transition, respectively.

Error bars for each data point depend on the uncertainties in the measured intensities and uncertainty in the noble gas density. The contributions to the uncertainty in each  $R_{J_i=1(G^1\Pi_g)}$  or  $R_{J_i=1(F^1\Sigma_g^+)}$  value, due to the uncertainty in the measured intensities, are calculated directly from

the expressions for  $R_{J_i=1(G^1\Pi_g)}$  or  $R_{J_i=1(F^1\Sigma_g^+)}$  in terms of the intensities Eq. (B1) or (B2) [Eq. (22) or (23) in the main text] according to

$$\begin{aligned} \Delta R_{J_i} &= \left| \frac{dR_{J_i}}{dI_{\text{Perp}}^{VH}} \right| \Delta I_{\text{Perp}}^{VH} + \left| \frac{dR_{J_i}}{dI_{\text{Par}}^{VH}} \right| \Delta I_{\text{Par}}^{VH} + \left| \frac{dR_{J_i}}{dI_{\text{Perp}}^{HV}} \right| \Delta I_{\text{Perp}}^{HV} \\ &+ \left| \frac{dR_{J_i}}{dI_{\text{Perp}}^{VV}} \right| \Delta I_{\text{Perp}}^{VV} + \left| \frac{dR_{J_i}}{dI_{\text{Par}}^{VV}} \right| \Delta I_{\text{Par}}^{VV} + \left| \frac{dR_{J_i}}{dI_{\text{Perp}}^{HH}} \right| \Delta I_{\text{Perp}}^{HH}. \end{aligned} \quad (\text{B3})$$

The derivatives are straightforward to calculate. From Eq. (B1) we obtain

$$\left| \frac{dR_{J_i=1(G^1\Pi_g)}}{dI_{\text{Perp}}^{VH}} \right| = \left| \frac{dR_{J_i=1(G^1\Pi_g)}}{dI_{\text{Par}}^{VH}} \right| = \left| \frac{dR_{J_i=1(G^1\Pi_g)}}{dI_{\text{Perp}}^{HV}} \right| = \left| \frac{2(I_{\text{Perp}}^{VV} + I_{\text{Par}}^{VV} + I_{\text{Perp}}^{HH})}{\left[ 2(I_{\text{Perp}}^{VH} + I_{\text{Par}}^{VH} + I_{\text{Perp}}^{HV}) - (I_{\text{Perp}}^{VV} + I_{\text{Par}}^{VV} + I_{\text{Perp}}^{HH}) \right]^2} \right|_{\text{Probe } J_i=1 \rightarrow G^1\Pi_g} \quad (\text{B4})$$

and

$$\left| \frac{dR_{J_i=1(G^1\Pi_g)}}{dI_{\text{Perp}}^{VV}} \right| = \left| \frac{dR_{J_i=1(G^1\Pi_g)}}{dI_{\text{Par}}^{VV}} \right| = \left| \frac{dR_{J_i=1(G^1\Pi_g)}}{dI_{\text{Perp}}^{HH}} \right| = \left| \frac{2(I_{\text{Perp}}^{VH} + I_{\text{Par}}^{VH} + I_{\text{Perp}}^{HV})}{\left[ 2(I_{\text{Perp}}^{VH} + I_{\text{Par}}^{VH} + I_{\text{Perp}}^{HV}) - (I_{\text{Perp}}^{VV} + I_{\text{Par}}^{VV} + I_{\text{Perp}}^{HH}) \right]^2} \right|_{\text{Probe } J_i=1 \rightarrow G^1\Pi_g} \quad (\text{B5})$$

Inserting these expressions into (B3) we find

$$\begin{aligned} \Delta R_{J_i=1(G^1\Pi_g)} &= \left| \frac{2(I_{\text{Perp}}^{VV} + I_{\text{Par}}^{VV} + I_{\text{Perp}}^{HH})}{\left[ 2(I_{\text{Perp}}^{VH} + I_{\text{Par}}^{VH} + I_{\text{Perp}}^{HV}) - (I_{\text{Perp}}^{VV} + I_{\text{Par}}^{VV} + I_{\text{Perp}}^{HH}) \right]^2} \right|_{\text{Probe } J_i=1 \rightarrow G^1\Pi_g} (\Delta I_{\text{Perp}}^{VH} + \Delta I_{\text{Par}}^{VH} + \Delta I_{\text{Perp}}^{HV}) \\ &+ \left| \frac{2(I_{\text{Perp}}^{VH} + I_{\text{Par}}^{VH} + I_{\text{Perp}}^{HV})}{\left[ 2(I_{\text{Perp}}^{VH} + I_{\text{Par}}^{VH} + I_{\text{Perp}}^{HV}) - (I_{\text{Perp}}^{VV} + I_{\text{Par}}^{VV} + I_{\text{Perp}}^{HH}) \right]^2} \right|_{\text{Probe } J_i=1 \rightarrow G^1\Pi_g} (\Delta I_{\text{Perp}}^{VV} + \Delta I_{\text{Par}}^{VV} + \Delta I_{\text{Perp}}^{HH}). \end{aligned} \quad (\text{B6})$$

Assuming that all the measured intensities have the same absolute uncertainty (this is a good approximation based on measured noise levels),

$$\Delta I_{\text{Perp}}^{VH} = \Delta I_{\text{Par}}^{VH} = \Delta I_{\text{Perp}}^{HV} = \Delta I_{\text{Perp}}^{VV} = \Delta I_{\text{Par}}^{VV} = \Delta I_{\text{Perp}}^{HH} \equiv \Delta I, \quad (\text{B7})$$

we find the contribution to  $\Delta R_{J_i=1(G^1\Pi_g)}$  due to the uncertainty in the measured intensities is

$$\begin{aligned} \Delta R_{J_i=1(G^1\Pi_g)} &= 6 \left| \frac{I_{\text{Perp}}^{VH} + I_{\text{Par}}^{VH} + I_{\text{Perp}}^{HV} + I_{\text{Perp}}^{VV} + I_{\text{Par}}^{VV} + I_{\text{Perp}}^{HH}}{\left[ 2 \left( I_{\text{Perp}}^{VH} + I_{\text{Par}}^{VH} + I_{\text{Perp}}^{HV} \right) - \left( I_{\text{Perp}}^{VV} + I_{\text{Par}}^{VV} + I_{\text{Perp}}^{HH} \right) \right]^2} \right|_{\text{Probe } J_i=1 \rightarrow G^1\Pi_g} \quad (\Delta I) \\ &= 6 \left| \frac{I^\perp + I^\parallel}{(2I^\perp - I^\parallel)^2} \right|_{\text{Probe } J_i=1 \rightarrow G^1\Pi_g} \quad (\Delta I). \end{aligned} \quad (\text{B8})$$

Similarly, using Eq. (B2) we calculate the derivatives in (B3) to obtain:

$$\left| \frac{dR_{J_i=1(F^1\Sigma_g^+)}}{dI_{\text{Perp}}^{VH}} \right| = \left| \frac{dR_{J_i=1(F^1\Sigma_g^+)}}{dI_{\text{Par}}^{VH}} \right| = \left| \frac{dR_{J_i=1(F^1\Sigma_g^+)}}{dI_{\text{Perp}}^{HV}} \right| = \left| \frac{1}{I_{\text{Perp}}^{VV} + I_{\text{Par}}^{VV} + I_{\text{Perp}}^{HH}} \right|_{\text{Probe } J_i=1 \rightarrow F^1\Sigma_g^+} \quad (\text{B9})$$

and

$$\left| \frac{dR_{J_i=1(F^1\Sigma_g^+)}}{dI_{\text{Perp}}^{VV}} \right| = \left| \frac{dR_{J_i=1(F^1\Sigma_g^+)}}{dI_{\text{Par}}^{VV}} \right| = \left| \frac{dR_{J_i=1(F^1\Sigma_g^+)}}{dI_{\text{Perp}}^{HH}} \right| = \left| \frac{I_{\text{Perp}}^{VH} + I_{\text{Par}}^{VH} + I_{\text{Perp}}^{HV}}{\left[ I_{\text{Perp}}^{VV} + I_{\text{Par}}^{VV} + I_{\text{Perp}}^{HH} \right]^2} \right|_{\text{Probe } J_i=1 \rightarrow F^1\Sigma_g^+} \quad (\text{B10})$$

Inserting these expressions into (B3) we find

$$\begin{aligned} \Delta R_{J_i=1(F^1\Sigma_g^+)} &= \left| \frac{1}{I_{\text{Perp}}^{VV} + I_{\text{Par}}^{VV} + I_{\text{Perp}}^{HH}} \right|_{\text{Probe } J_i=1 \rightarrow F^1\Sigma_g^+} \left( \Delta I_{\text{Perp}}^{VH} + \Delta I_{\text{Par}}^{VH} + \Delta I_{\text{Perp}}^{HV} \right) \\ &+ \left| \frac{I_{\text{Perp}}^{VH} + I_{\text{Par}}^{VH} + I_{\text{Perp}}^{HV}}{\left[ I_{\text{Perp}}^{VV} + I_{\text{Par}}^{VV} + I_{\text{Perp}}^{HH} \right]^2} \right|_{\text{Probe } J_i=1 \rightarrow F^1\Sigma_g^+} \left( \Delta I_{\text{Perp}}^{VV} + \Delta I_{\text{Par}}^{VV} + \Delta I_{\text{Perp}}^{HH} \right). \end{aligned} \quad (\text{B11})$$

Again, assuming that all the measured intensities have the same absolute uncertainty (B7), we find the contribution to  $\Delta R_{J_i=1(F^1\Sigma_g^+)}$  due to the uncertainty in the measured intensities is

$$\Delta R_{J_i=1(F^1\Sigma_g^+)} = 3 \left| \frac{I_{\text{Perp}}^{VH} + I_{\text{Par}}^{VH} + I_{\text{Perp}}^{HV} + I_{\text{Perp}}^{VV} + I_{\text{Par}}^{VV} + I_{\text{Perp}}^{HH}}{\left[ I_{\text{Perp}}^{VV} + I_{\text{Par}}^{VV} + I_{\text{Perp}}^{HH} \right]^2} \right|_{\text{Probe } J_i=1 \rightarrow F^1\Sigma_g^+} \quad (\Delta I)$$

$$= 3 \left| \frac{I^\perp + I^\parallel}{(I^\parallel)^2} \right|_{\text{Probe } J_i=1 \rightarrow F^1\Sigma_g^+} \quad (\Delta I).$$

(B12)

For  $J$ -changing data obtained using the  $G^1\Pi_g (v_e = 5, J_e = J_i) \leftarrow A^1\Sigma_u^+ (v_i = 5, J_i = 3, 5, 7)$  and  $G^1\Pi_g (v_e = 5, J'_e = J'_i) \leftarrow A^1\Sigma_u^+ (v_i = 5, J'_i = 1)$  probe transitions, the fitting function is given by Eqs. (24) in the published manuscript:

$$R_{J_i=3,5,7} \equiv \frac{\left[ 2I^\perp + I^\parallel \right]_{\text{Probe } J_i=3,5,7 \rightarrow G^1\Pi_g}}{\left[ 2I^\perp + I^\parallel \right]_{\text{Probe } J'_i=1 \rightarrow G^1\Pi_g}} \equiv \frac{\left[ 2(I_{\text{Perp}}^{VH} + I_{\text{Par}}^{VH} + I_{\text{Perp}}^{HV}) + (I_{\text{Perp}}^{VV} + I_{\text{Par}}^{VV} + I_{\text{Perp}}^{HH}) \right]_{\text{Probe } J_i=3,5,7 \rightarrow G^1\Pi_g}}{\left[ 2(I_{\text{Perp}}^{VH} + I_{\text{Par}}^{VH} + I_{\text{Perp}}^{HV}) + (I_{\text{Perp}}^{VV} + I_{\text{Par}}^{VV} + I_{\text{Perp}}^{HH}) \right]_{\text{Probe } J'_i=1 \rightarrow G^1\Pi_g}}$$

$$= \frac{\left[ \tilde{k}_{NG}^{J'_i=1 \rightarrow J_i=3,5,7} n_{NG} + C_{3,5,7} \right]}{1 + \tilde{k}_{NG}^Q n_{NG} + C_Q}.$$

(B13)

In this case, we must consider derivatives with respect to twelve different intensities (six when probing  $J_i = 3, 5, \text{ or } 7$  and six when probing  $J'_i = 1$ ). The necessary derivatives are

$$\left| \frac{dR_{J_i=3,5,7}}{d(I_{\text{Perp}}^{VH})_{\text{Probe } J_i=3,5,7 \rightarrow G^1\Pi_g}} \right| = \left| \frac{dR_{J_i=3,5,7}}{d(I_{\text{Par}}^{VH})_{\text{Probe } J_i=3,5,7 \rightarrow G^1\Pi_g}} \right| = \left| \frac{dR_{J_i=3,5,7}}{d(I_{\text{Perp}}^{HV})_{\text{Probe } J_i=3,5,7 \rightarrow G^1\Pi_g}} \right|$$

$$= \left| \frac{2}{\left[ 2(I_{\text{Perp}}^{VH} + I_{\text{Par}}^{VH} + I_{\text{Perp}}^{HV}) + (I_{\text{Perp}}^{VV} + I_{\text{Par}}^{VV} + I_{\text{Perp}}^{HH}) \right]_{\text{Probe } J'_i=1 \rightarrow G^1\Pi_g}} \right|,$$

(B14)

$$\begin{aligned}
& \left| \frac{dR_{J_i=3,5,7}}{d(I_{\text{Perp}}^{VV})_{\text{Probe } J_i=3,5,7 \rightarrow G^1 \Pi_g}} \right| = \left| \frac{dR_{J_i=3,5,7}}{d(I_{\text{Par}}^{VV})_{\text{Probe } J_i=3,5,7 \rightarrow G^1 \Pi_g}} \right| = \left| \frac{dR_{J_i=3,5,7}}{d(I_{\text{Perp}}^{HH})_{\text{Probe } J_i=3,5,7 \rightarrow G^1 \Pi_g}} \right| \\
& = \left| \frac{1}{\left[ 2(I_{\text{Perp}}^{VH} + I_{\text{Par}}^{VH} + I_{\text{Perp}}^{HV}) + (I_{\text{Perp}}^{VV} + I_{\text{Par}}^{VV} + I_{\text{Perp}}^{HH}) \right]_{\text{Probe } J'_i=1 \rightarrow G^1 \Pi_g}} \right|,
\end{aligned} \tag{B15}$$

$$\begin{aligned}
& \left| \frac{dR_{J_i=3,5,7}}{d(I_{\text{Perp}}^{VH})_{\text{Probe } J'_i=1 \rightarrow G^1 \Pi_g}} \right| = \left| \frac{dR_{J_i=3,5,7}}{d(I_{\text{Par}}^{VH})_{\text{Probe } J'_i=1 \rightarrow G^1 \Pi_g}} \right| = \left| \frac{dR_{J_i=3,5,7}}{d(I_{\text{Perp}}^{HV})_{\text{Probe } J'_i=1 \rightarrow G^1 \Pi_g}} \right| \\
& = \left| \frac{2 \left[ 2(I_{\text{Perp}}^{VH} + I_{\text{Par}}^{VH} + I_{\text{Perp}}^{HV}) + (I_{\text{Perp}}^{VV} + I_{\text{Par}}^{VV} + I_{\text{Perp}}^{HH}) \right]_{\text{Probe } J_i=3,5,7 \rightarrow G^1 \Pi_g}}{\left[ 2(I_{\text{Perp}}^{VH} + I_{\text{Par}}^{VH} + I_{\text{Perp}}^{HV}) + (I_{\text{Perp}}^{VV} + I_{\text{Par}}^{VV} + I_{\text{Perp}}^{HH}) \right]_{\text{Probe } J'_i=1 \rightarrow G^1 \Pi_g}^2} \right|,
\end{aligned} \tag{B16}$$

and

$$\begin{aligned}
& \left| \frac{dR_{J_i=3,5,7}}{d(I_{\text{Perp}}^{VV})_{\text{Probe } J'_i=1 \rightarrow G^1 \Pi_g}} \right| = \left| \frac{dR_{J_i=3,5,7}}{d(I_{\text{Par}}^{VV})_{\text{Probe } J'_i=1 \rightarrow G^1 \Pi_g}} \right| = \left| \frac{dR_{J_i=3,5,7}}{d(I_{\text{Perp}}^{HH})_{\text{Probe } J'_i=1 \rightarrow G^1 \Pi_g}} \right| \\
& = \left| \frac{\left[ 2(I_{\text{Perp}}^{VH} + I_{\text{Par}}^{VH} + I_{\text{Perp}}^{HV}) + (I_{\text{Perp}}^{VV} + I_{\text{Par}}^{VV} + I_{\text{Perp}}^{HH}) \right]_{\text{Probe } J_i=3,5,7 \rightarrow G^1 \Pi_g}}{\left[ 2(I_{\text{Perp}}^{VH} + I_{\text{Par}}^{VH} + I_{\text{Perp}}^{HV}) + (I_{\text{Perp}}^{VV} + I_{\text{Par}}^{VV} + I_{\text{Perp}}^{HH}) \right]_{\text{Probe } J'_i=1 \rightarrow G^1 \Pi_g}^2} \right|.
\end{aligned} \tag{B17}$$

Inserting these into an appropriately modified version of (B3) yields

$$\begin{aligned}
& \Delta R_{J_i=3,5,7} \\
&= \left| \frac{1}{\left[ 2(I_{\text{Perp}}^{VH} + I_{\text{Par}}^{VH} + I_{\text{Perp}}^{HV}) + (I_{\text{Perp}}^{VV} + I_{\text{Par}}^{VV} + I_{\text{Perp}}^{HH}) \right]_{\text{Probe } J'_i=1 \rightarrow G^1 \Pi_g}} \right| \\
& \times \left[ 2(\Delta I_{\text{Perp}}^{VH} + \Delta I_{\text{Par}}^{VH} + \Delta I_{\text{Perp}}^{HV}) + (\Delta I_{\text{Perp}}^{VV} + \Delta I_{\text{Par}}^{VV} + \Delta I_{\text{Perp}}^{HH}) \right]_{\text{Probe } J_i=3,5,7 \rightarrow G^1 \Pi_g} \\
& + \left| \frac{\left[ 2(I_{\text{Perp}}^{VH} + I_{\text{Par}}^{VH} + I_{\text{Perp}}^{HV}) + (I_{\text{Perp}}^{VV} + I_{\text{Par}}^{VV} + I_{\text{Perp}}^{HH}) \right]_{\text{Probe } J_i=3,5,7 \rightarrow G^1 \Pi_g}}{\left[ 2(I_{\text{Perp}}^{VH} + I_{\text{Par}}^{VH} + I_{\text{Perp}}^{HV}) + (I_{\text{Perp}}^{VV} + I_{\text{Par}}^{VV} + I_{\text{Perp}}^{HH}) \right]_{\text{Probe } J'_i=1 \rightarrow G^1 \Pi_g}^2} \right| \\
& \times \left[ 2(\Delta I_{\text{Perp}}^{VH} + \Delta I_{\text{Par}}^{VH} + \Delta I_{\text{Perp}}^{HV}) + (\Delta I_{\text{Perp}}^{VV} + \Delta I_{\text{Par}}^{VV} + \Delta I_{\text{Perp}}^{HH}) \right]_{\text{Probe } J'_i=1 \rightarrow G^1 \Pi_g}.
\end{aligned} \tag{B18}$$

Again, assuming that all the measured intensities have the same absolute uncertainty (B7), we find the contribution to  $\Delta R_{J_i=3,5,7}$  due to the uncertainty in the measured intensities is

$$\begin{aligned}
\Delta R_{J_i=3,5,7} &= 9 \left| \frac{\left\{ \left[ 2(I_{\text{Perp}}^{VH} + I_{\text{Par}}^{VH} + I_{\text{Perp}}^{HV}) + (I_{\text{Perp}}^{VV} + I_{\text{Par}}^{VV} + I_{\text{Perp}}^{HH}) \right]_{\text{Probe } J_i=3,5,7 \rightarrow G^1 \Pi_g} \right. \right. \\
& \quad \left. \left. + \left[ 2(I_{\text{Perp}}^{VH} + I_{\text{Par}}^{VH} + I_{\text{Perp}}^{HV}) + (I_{\text{Perp}}^{VV} + I_{\text{Par}}^{VV} + I_{\text{Perp}}^{HH}) \right]_{\text{Probe } J'_i=1 \rightarrow G^1 \Pi_g} \right\}}{\left[ 2(I_{\text{Perp}}^{VH} + I_{\text{Par}}^{VH} + I_{\text{Perp}}^{HV}) + (I_{\text{Perp}}^{VV} + I_{\text{Par}}^{VV} + I_{\text{Perp}}^{HH}) \right]_{\text{Probe } J'_i=1 \rightarrow G^1 \Pi_g}^2} \right| (\Delta I) \\
&= 9 \left| \frac{\left[ 2I^\perp + I^\parallel \right]_{\text{Probe } J_i=3,5,7 \rightarrow G^1 \Pi_g} + \left[ 2I^\perp + I^\parallel \right]_{\text{Probe } J'_i=1 \rightarrow G^1 \Pi_g}}{\left[ 2I^\perp + I^\parallel \right]_{\text{Probe } J'_i=1 \rightarrow G^1 \Pi_g}^2} \right| (\Delta I).
\end{aligned} \tag{B19}$$

The right hand sides of Eqs. (B1), (B2), and (B13) [Eqs. (22), (23), and (24) of the main text] are all of the same form. Therefore, the contribution to the uncertainty in each  $R_{J_i=(G^1 \Pi_g)}$  and  $R_{J_i=(F^1 \Sigma_g^+)}$  value due to the uncertainty in the noble gas density is calculated using the right hand side of Eqs. (B1) and (B2) according to

$$\begin{aligned}
\left| \frac{dR_{J_i=1}}{dn_{NG}} \right| \Delta n_{NG} &= \left| \frac{\tilde{k}_{NG}^{J_i=1, M_i=0 \rightarrow \pm 1}}{1 + \tilde{k}_{NG}^Q n_{NG} + C_Q} - \frac{\tilde{k}_{NG}^Q (\tilde{k}_{NG}^{J_i=1, M_i=0 \rightarrow \pm 1} n_{NG} + C_1)}{(1 + \tilde{k}_{NG}^Q n_{NG} + C_Q)^2} \right| \Delta n_{NG} \\
&= \left| \frac{\tilde{k}_{NG}^{J_i=1, M_i=0 \rightarrow \pm 1}}{(\tilde{k}_{NG}^{J_i=1, M_i=0 \rightarrow \pm 1} n_{NG} + C_1)} - \frac{\tilde{k}_{NG}^Q}{(1 + \tilde{k}_{NG}^Q n_{NG} + C_Q)} \right| \left( \frac{\tilde{k}_{NG}^{J_i=1, M_i=0 \rightarrow \pm 1} n_{NG} + C_1}{1 + \tilde{k}_{NG}^Q n_{NG} + C_Q} \right) \Delta n_{NG}.
\end{aligned} \tag{B20}$$

Combining the contributions from the uncertainties in the intensities (B8) or (B12) with those from the uncertainty in the noble gas density (B20), we obtain

$$\begin{aligned}
\Delta R_{J_i=1(G^1\Pi_g)} &= \left| \frac{\tilde{k}_{NG}^{J_i=1, M_i=0 \rightarrow \pm 1}}{(\tilde{k}_{NG}^{J_i=1, M_i=0 \rightarrow \pm 1} n_{NG} + C_1)} - \frac{\tilde{k}_{NG}^Q}{(1 + \tilde{k}_{NG}^Q n_{NG} + C_Q)} \right| \left( \frac{\tilde{k}_{NG}^{J_i=1, M_i=0 \rightarrow \pm 1} n_{NG} + C_1}{1 + \tilde{k}_{NG}^Q n_{NG} + C_Q} \right) \Delta n_{NG} \\
&\quad + 6 \left| \frac{I^\perp + I^\parallel}{(2I^\perp - I^\parallel)^2} \right|_{\text{Probe } J_i=1 \rightarrow G^1\Pi_g} (\Delta I)
\end{aligned} \tag{B21}$$

and

$$\begin{aligned}
\Delta R_{J_i=1(F^1\Sigma_g^+)} &= \left| \frac{\tilde{k}_{NG}^{J_i=1, M_i=0 \rightarrow \pm 1}}{(\tilde{k}_{NG}^{J_i=1, M_i=0 \rightarrow \pm 1} n_{NG} + C_1)} - \frac{\tilde{k}_{NG}^Q}{(1 + \tilde{k}_{NG}^Q n_{NG} + C_Q)} \right| \left( \frac{\tilde{k}_{NG}^{J_i=1, M_i=0 \rightarrow \pm 1} n_{NG} + C_1}{1 + \tilde{k}_{NG}^Q n_{NG} + C_Q} \right) \Delta n_{NG} \\
&\quad + 3 \left| \frac{I^\perp + I^\parallel}{(I^\parallel)^2} \right|_{\text{Probe } J_i=1 \rightarrow F^1\Sigma_g^+} (\Delta I).
\end{aligned} \tag{B22}$$

For the  $J$ -changing data, a similar calculation of  $\left| \frac{dR_{J_i=3,5,7}}{dn_{NG}} \right| \Delta n_{NG}$  yields

$$\begin{aligned}
\left| \frac{dR_{J_i=3,5,7}}{dn_{NG}} \right| \Delta n_{NG} &= \left| \frac{\tilde{k}_{NG}^{J'_i=1 \rightarrow J_i=3,5,7}}{1 + \tilde{k}_{NG}^Q n_{NG} + C_Q} - \frac{\tilde{k}_{NG}^Q (\tilde{k}_{NG}^{J'_i=1 \rightarrow J_i=3,5,7} n_{NG} + C_{3,5,7})}{(1 + \tilde{k}_{NG}^Q n_{NG} + C_Q)^2} \right| \Delta n_{NG} \\
&= \left| \frac{\tilde{k}_{NG}^{J'_i=1 \rightarrow J_i=3,5,7}}{(\tilde{k}_{NG}^{J'_i=1 \rightarrow J_i=3,5,7} n_{NG} + C_{3,5,7})} - \frac{\tilde{k}_{NG}^Q}{(1 + \tilde{k}_{NG}^Q n_{NG} + C_Q)} \right| \left( \frac{(\tilde{k}_{NG}^{J'_i=1 \rightarrow J_i=3,5,7} n_{NG} + C_{3,5,7})}{1 + \tilde{k}_{NG}^Q n_{NG} + C_Q} \right) \Delta n_{NG},
\end{aligned} \tag{B23}$$

and hence

$$\begin{aligned}
\Delta R_{J_i=3,5,7} &= \left| \frac{\tilde{k}_{NG}^{J'_i=1 \rightarrow J_i=3,5,7}}{(\tilde{k}_{NG}^{J'_i=1 \rightarrow J_i=3,5,7} n_{NG} + C_{3,5,7})} - \frac{\tilde{k}_{NG}^Q}{(1 + \tilde{k}_{NG}^Q n_{NG} + C_Q)} \right| \left( \frac{(\tilde{k}_{NG}^{J'_i=1 \rightarrow J_i=3,5,7} n_{NG} + C_{3,5,7})}{1 + \tilde{k}_{NG}^Q n_{NG} + C_Q} \right) \Delta n_{NG} \\
&\quad + 9 \left| \frac{\left[ 2I^\perp + I^\parallel \right]_{\text{Probe } J_i=3,5,7 \rightarrow G^1\Pi_g} + \left[ 2I^\perp + I^\parallel \right]_{\text{Probe } J'_i=1 \rightarrow G^1\Pi_g}}{\left[ 2I^\perp + I^\parallel \right]_{\text{Probe } J'_i=1 \rightarrow G^1\Pi_g}^2} \right| (\Delta I).
\end{aligned} \tag{B24}$$

### Appendix C – Results from the fits using the “single collision approximation”

Using the single collision approximation as described in Section III.C.i. of the main text, we simultaneously fit all of the argon and helium data with Eqs. (22), (23), and (24) for the  $M$ -changing data obtained using the  $G^1\Pi_g(v_e=5, J_e=J_i=1) \leftarrow A^1\Sigma_u^+(v_i=5, J_i=1)$  probe transition,  $M$ -changing data obtained using the  $F^1\Sigma_g^+(v_e=12, J_e=0) \leftarrow A^1\Sigma_u^+(v_i=5, J_i=1)$  probe transition, and  $J$ -changing data obtained using the  $G^1\Pi_g(v_e=5, J_e=J_i) \leftarrow A^1\Sigma_u^+(v_i=5, J_i=3, 5, 7)$  and  $G^1\Pi_g(v_e=5, J'_e=J'_i) \leftarrow A^1\Sigma_u^+(v_i=5, J'_i=1)$  probe transitions, respectively, with weightings given in Eqs. (26), (27), and (28) [(B21), (B22), and (B24)], respectively. As explained in the text, the lithium parameters  $C_1$ ,  $C_3$ ,  $C_5$ ,  $C_7$ , and  $C_Q$  were all set to zero in this fit. Results are given in Table C.1 and the data are plotted against the fitting functions in Figs. C.1 and C.2 here. Note that these results are not the “final” values since they do not include multiple collision corrections. The latter are discussed in Sec. III.C.ii of the main text.

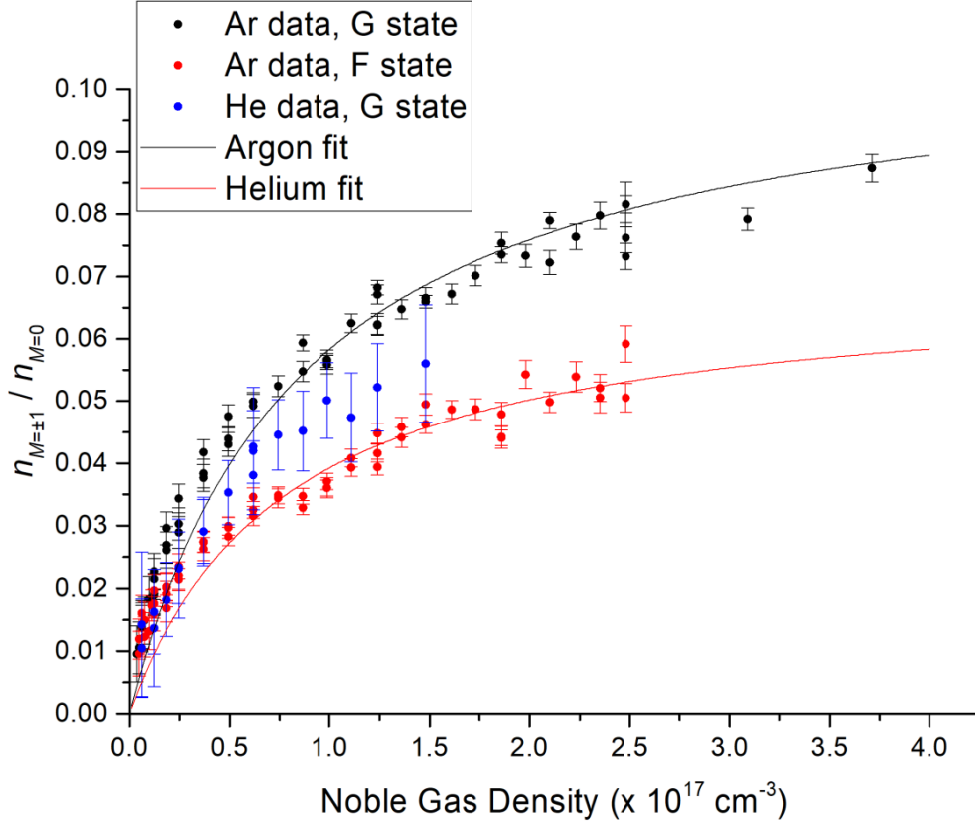


Figure C.1. Data and fitting function for elastic ( $M$ -changing) collisions of  $\text{Li}_2$   $A^1\Sigma_u^+(v_i=5, J_i=1)$  molecules with noble gas atoms. The plot shows the density in either collisionally populated level  $J_i=1, M_i=+1$  or  $J_i=1, M_i=-1$  divided by the density in the directly excited level  $J_i=1, M_i=0$  vs. noble gas density. Black and red data points were recorded using the  $G^1\Pi_g(v_e=5, J_e=J_i=1) \leftarrow A^1\Sigma_u^+(v_i=5, J_i=1)$  probe transition with argon or helium buffer gas, respectively. Blue data points were recorded using the  $F^1\Sigma_g^+(v_e=12, J_e=0) \leftarrow A^1\Sigma_u^+(v_i=5, J_i=1)$  probe transition with argon buffer gas. The black curve is a fit to all argon data (including both probe transitions), while the red curve is a fit to the helium data. These fits were obtained using the analysis based on the single collision approximation. Final results based on the more complete model that includes multiple collision effects are shown in Figs. 6 and 7 of the main text.

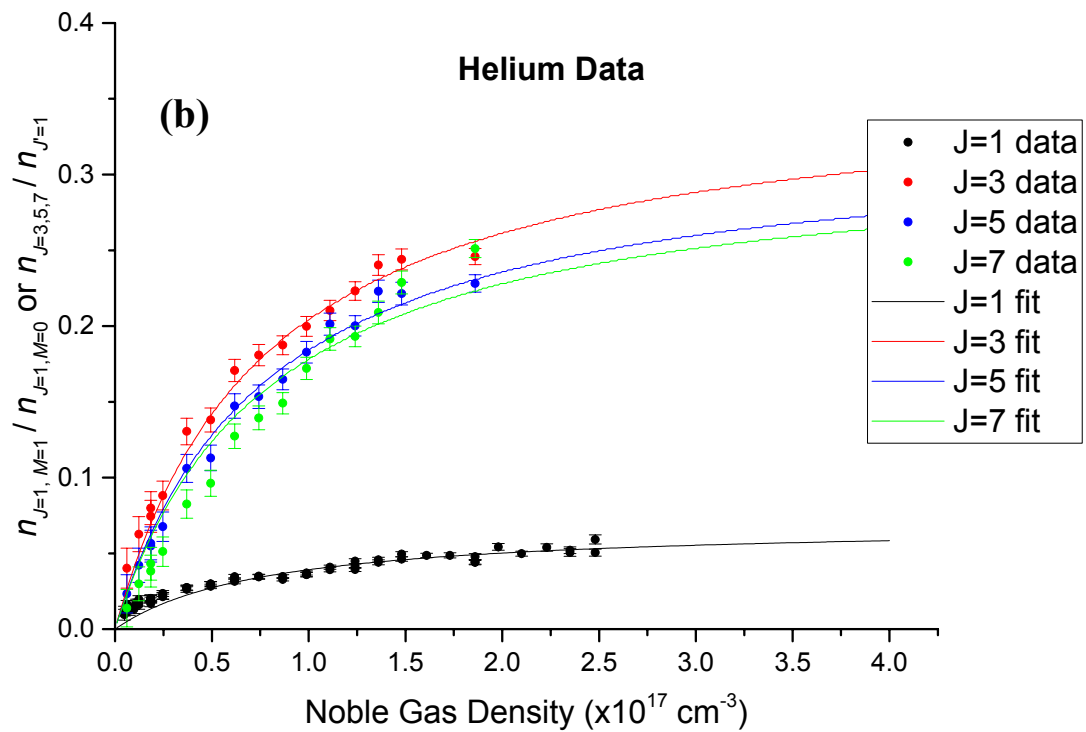
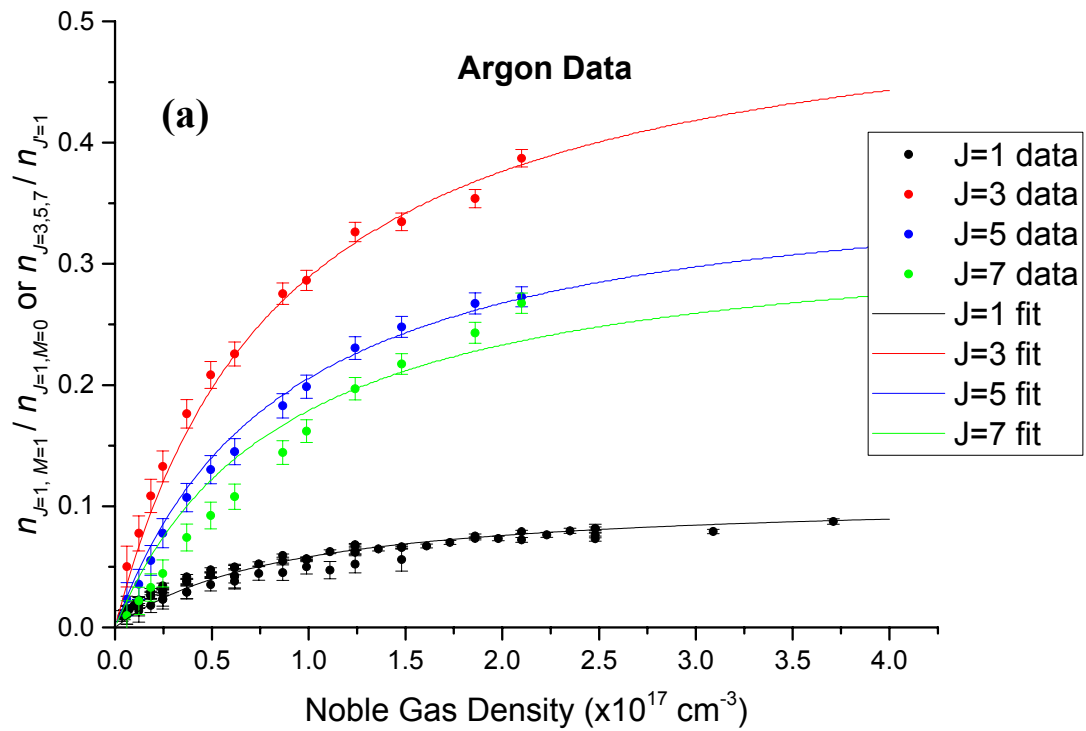


Figure C.2. Data and fitting function for elastic ( $M$ -changing) and inelastic ( $J$ -changing) collisions of  $\text{Li}_2 A^1\Sigma_u^+(v_i=5, J_i=1)$  molecules with noble gas atoms. The black data points show the density in either collisionally populated level  $J_i=1, M_i=+1$  or  $J_i=1, M_i=-1$  divided by the density in the directly excited level  $J_i=1, M_i=0$  vs. noble gas density. Red, blue, and green data points show the density in the collisionally populated levels  $J_i=3, 5,$  or  $7,$  respectively, divided by the density in the directly excited level  $J_i=1$  vs. noble gas density. The red, blue, and green solid lines represent fits obtained using the analysis based on the single collision approximation for  $J_i=3, 5,$  or  $7,$  respectively. Final results based on the more complete model that includes multiple collision effects are shown in Figs. 6 and 7 of the main text. (a) Argon data, (b) Helium data.

Table C.1 – Preliminary values of rate coefficients ( $k_{Ar,He}^{J_i=1,M_i=0 \rightarrow \pm 1}$  and  $k_{Ar,He}^{J'_i=1 \rightarrow J_i=3,5,7}$ ) divided by the radiative rate  $\Gamma$  and in units of  $\text{cm}^3\text{s}^{-1}$  [the latter obtained by multiplying the fitted parameters ( $\tilde{k}_{Ar,He}^{J_i=1,M_i=0 \rightarrow \pm 1}$  and  $\tilde{k}_{Ar,He}^{J'_i=1 \rightarrow J_i=3,5,7}$ ) by  $\Gamma = 5.45 \times 10^7 \text{ s}^{-1}$  [8]] for  $M$ -changing (elastic) collisions,  $A^1\Sigma_u^+(v_i = 5, J_i = 1, M_i = 0) \rightarrow A^1\Sigma_u^+(v_i = 5, J_i = 1, M_i = \pm 1)$ , and for  $J$ -changing (inelastic) collisions,  $A^1\Sigma_u^+(v_i = 5, J'_i = 1) \rightarrow A^1\Sigma_u^+(v_i = 5, J_i = 3, 5, 7)$ , of  $\text{Li}_2$  molecules with argon and helium atoms. Quenching rate coefficients are also given. Note that these results are based on the single collision approximation that is not a good approximation for the higher pressure  $J$ -changing collision data. Quoted uncertainties represent statistical errors only. Systematic errors due to neglect of multiple collision effects are much larger. Final values, corrected for multiple collision effects, are given in Table I of the main text.

$M$ -changing	$\tilde{k}_{Ar}^{J_i=1,M_i=0 \rightarrow \pm 1}$ ( $10^{-18} \text{ cm}^3$ )	$\tilde{k}_{He}^{J_i=1,M_i=0 \rightarrow \pm 1}$ ( $10^{-18} \text{ cm}^3$ )	$k_{Ar}^{J_i=1,M_i=0 \rightarrow \pm 1}$ ( $10^{-11} \text{ cm}^3\text{s}^{-1}$ )	$k_{He}^{J_i=1,M_i=0 \rightarrow \pm 1}$ ( $10^{-11} \text{ cm}^3\text{s}^{-1}$ )	
	$J_i = 1, M_i = 0 \rightarrow J_i = 1, M_i = \pm 1$	1.26 $\pm$ 0.05	0.90 $\pm$ 0.05	6.85 $\pm$ 0.26	4.89 $\pm$ 0.25
$J$ -changing	$\tilde{k}_{Ar}^{J'_i=1 \rightarrow J_i=3,5,7}$ ( $10^{-18} \text{ cm}^3$ )	$\tilde{k}_{He}^{J'_i=1 \rightarrow J_i=3,5,7}$ ( $10^{-18} \text{ cm}^3$ )	$k_{Ar}^{J'_i=1 \rightarrow J_i=3,5,7}$ ( $10^{-11} \text{ cm}^3\text{s}^{-1}$ )	$k_{He}^{J'_i=1 \rightarrow J_i=3,5,7}$ ( $10^{-11} \text{ cm}^3\text{s}^{-1}$ )	
	$J'_i = 1 \rightarrow J_i = 3$	6.23 $\pm$ 0.24	4.67 $\pm$ 0.24	33.9 $\pm$ 1.3	25.4 $\pm$ 1.3
	$J'_i = 1 \rightarrow J_i = 5$	4.43 $\pm$ 0.17	4.21 $\pm$ 0.21	24.1 $\pm$ 0.9	22.9 $\pm$ 1.2
	$J'_i = 1 \rightarrow J_i = 7$	3.86 $\pm$ 0.15	4.07 $\pm$ 0.21	21.0 $\pm$ 0.8	22.2 $\pm$ 1.1
Quenching	$\tilde{k}_{Ar}^Q$ ( $10^{-18} \text{ cm}^3$ )	$\tilde{k}_{He}^Q$ ( $10^{-18} \text{ cm}^3$ )	$k_{Ar}^Q$ ( $10^{-11} \text{ cm}^3\text{s}^{-1}$ )	$k_{He}^Q$ ( $10^{-11} \text{ cm}^3\text{s}^{-1}$ )	
	11.5 $\pm$ 0.7	12.9 $\pm$ 1.0	62.9 $\pm$ 3.7	70.1 $\pm$ 5.6	

## Appendix D – Multiple collision corrections

Starting from Eq. (29) of the main text, and truncating the sum at  $J \leq 7$  we obtain the following set of equations:

$$\left(1 + \tilde{k}_{NG}^{Q, J_i=3} n_{NG}\right) \frac{n_{J_i=3}}{n_{J_i=1}} - \left(\tilde{k}_{NG}^{J=5 \rightarrow J_i=3} n_{NG}\right) \frac{n_{J_i=5}}{n_{J_i=1}} - \left(\tilde{k}_{NG}^{J=7 \rightarrow J_i=3} n_{NG}\right) \frac{n_{J_i=7}}{n_{J_i=1}} = \tilde{k}_{NG}^{J_i=1 \rightarrow J_i=3} n_{NG} \cdot \quad (D1)$$

$$-\left(\tilde{k}_{NG}^{J=3 \rightarrow J_i=5} n_{NG}\right) \frac{n_{J_i=3}}{n_{J_i=1}} + \left(1 + \tilde{k}_{NG}^{Q, J_i=5} n_{NG}\right) \frac{n_{J_i=5}}{n_{J_i=1}} - \left(\tilde{k}_{NG}^{J=7 \rightarrow J_i=5} n_{NG}\right) \frac{n_{J_i=7}}{n_{J_i=1}} = \tilde{k}_{NG}^{J_i=1 \rightarrow J_i=5} n_{NG} \quad (D2)$$

and

$$-\left(\tilde{k}_{NG}^{J=3 \rightarrow J_i=7} n_{NG}\right) \frac{n_{J_i=3}}{n_{J_i=1}} - \left(\tilde{k}_{NG}^{J=5 \rightarrow J_i=7} n_{NG}\right) \frac{n_{J_i=5}}{n_{J_i=1}} + \left(1 + \tilde{k}_{NG}^{Q, J_i=7} n_{NG}\right) \frac{n_{J_i=7}}{n_{J_i=1}} = \tilde{k}_{NG}^{J_i=1 \rightarrow J_i=7} n_{NG} \cdot \quad (D3)$$

As discussed in the main text after Eq. (29), we introduce the assumption that  $k_{NG}^{J=3 \rightarrow J_i=5} = k_{NG}^{J=5 \rightarrow J_i=7} = k_{NG}^{J_i=1 \rightarrow J_i=3}$  since these all correspond to  $\Delta J = 2$  collisions, and  $k_{NG}^{J=3 \rightarrow J_i=7} = k_{NG}^{J_i=1 \rightarrow J_i=5}$  since these both correspond to  $\Delta J = 4$ , and we set  $k_{NG}^{J=5 \rightarrow J_i=3} = (7/11) k_{NG}^{J=3 \rightarrow J_i=5} = (7/11) k_{NG}^{J_i=1 \rightarrow J_i=3}$ ,  $k_{NG}^{J=7 \rightarrow J_i=5} = (11/15) k_{NG}^{J=5 \rightarrow J_i=7} = (11/15) k_{NG}^{J_i=1 \rightarrow J_i=3}$ , and  $k_{NG}^{J=7 \rightarrow J_i=3} = (7/15) k_{NG}^{J=3 \rightarrow J_i=7} = (7/15) k_{NG}^{J_i=1 \rightarrow J_i=5}$  from the principle of detailed balance. Finally, we make the same approximations that were used in the single collision analysis; i.e., that the radiative decay rates and quenching rate coefficients are the same for the four levels under investigation. Consequently, Eqs. (D1)-(D3) reduce to

$$\left(1 + \tilde{k}_{NG}^Q n_{NG}\right) \frac{n_{J_i=3}}{n_{J_i=1}} - \left(\frac{7}{11} \tilde{k}_{NG}^{J_i=1 \rightarrow J_i=3} n_{NG}\right) \frac{n_{J_i=5}}{n_{J_i=1}} - \left(\frac{7}{15} \tilde{k}_{NG}^{J_i=1 \rightarrow J_i=5} n_{NG}\right) \frac{n_{J_i=7}}{n_{J_i=1}} = \tilde{k}_{NG}^{J_i=1 \rightarrow J_i=3} n_{NG} \quad (D4)$$

$$-\left(\tilde{k}_{NG}^{J_i=1 \rightarrow J_i=3} n_{NG}\right) \frac{n_{J_i=3}}{n_{J_i=1}} + \left(1 + \tilde{k}_{NG}^Q n_{NG}\right) \frac{n_{J_i=5}}{n_{J_i=1}} - \left(\frac{11}{15} \tilde{k}_{NG}^{J_i=1 \rightarrow J_i=3} n_{NG}\right) \frac{n_{J_i=7}}{n_{J_i=1}} = \tilde{k}_{NG}^{J_i=1 \rightarrow J_i=5} n_{NG} \quad (D5)$$

and

$$-\left(\tilde{k}_{NG}^{J_i=1 \rightarrow J_i=5} n_{NG}\right) \frac{n_{J_i=3}}{n_{J_i=1}} - \left(\tilde{k}_{NG}^{J_i=1 \rightarrow J_i=3} n_{NG}\right) \frac{n_{J_i=5}}{n_{J_i=1}} + \left(1 + \tilde{k}_{NG}^Q n_{NG}\right) \frac{n_{J_i=7}}{n_{J_i=1}} = \tilde{k}_{NG}^{J_i=1 \rightarrow J_i=7} n_{NG} \cdot \quad (D6)$$

Now we have three equations for three unknown density ratios  $n_{J_i=3}/n_{J_i=1}$ ,  $n_{J_i=5}/n_{J_i=1}$ , and  $n_{J_i=7}/n_{J_i=1}$ . Using the following shorthand notation

$$z_{13} \equiv \left( \tilde{k}_{NG}^{J'_i=1 \rightarrow J_i=3} n_{NG} \right), \quad (\text{D7})$$

$$z_{15} \equiv \left( \tilde{k}_{NG}^{J'_i=1 \rightarrow J_i=5} n_{NG} \right), \quad (\text{D8})$$

$$z_{17} \equiv \left( \tilde{k}_{NG}^{J'_i=1 \rightarrow J_i=7} n_{NG} \right), \quad (\text{D9})$$

and

$$Q \equiv \left( 1 + \tilde{k}_{NG}^Q n_{NG} \right), \quad (\text{D10})$$

we can write the solutions to Eqs. (D4)-(D6) as

$$\frac{n_{J_i=3}}{n_{J'_i=1}} = \left[ \frac{165Q^2 z_{13} + 105Q z_{13} z_{15} + 77Q z_{15} z_{17} - 121z_{13}^3 + 77z_{13}^2 z_{17} + 77z_{13} z_{15}^2}{165Q^3 - 226Q z_{13}^2 - 77Q z_{15}^2 - 154z_{13}^2 z_{15}} \right], \quad (\text{D11})$$

$$\frac{n_{J_i=5}}{n_{J'_i=1}} = \left[ \frac{165Q^2 z_{15} + 165Q z_{13}^2 + 121Q z_{13} z_{17} + 121z_{13}^2 z_{15} + 77z_{13} z_{15} z_{17} - 77z_{15}^3}{165Q^3 - 226Q z_{13}^2 - 77Q z_{15}^2 - 154z_{13}^2 z_{15}} \right], \quad (\text{D12})$$

and

$$\frac{n_{J_i=7}}{n_{J'_i=1}} = \left[ \frac{165Q^2 z_{17} + 330Q z_{13} z_{15} + 165z_{13}^3 - 105z_{13}^2 z_{17} + 105z_{13} z_{15}^2}{165Q^3 - 226Q z_{13}^2 - 77Q z_{15}^2 - 154z_{13}^2 z_{15}} \right]. \quad (\text{D13})$$

As before, the density ratios are related to the measured intensity ratios by

$$\frac{n_{J_i=3}}{n_{J'_i=1}} = \frac{\left[ 2I^\perp + I^\parallel \right]_{\text{Probe } J_i=3 \rightarrow G^1 \Pi_g}}{\left[ 2I^\perp + I^\parallel \right]_{\text{Probe } J'_i=1 \rightarrow G^1 \Pi_g}}, \quad (\text{D14})$$

$$\frac{n_{J_i=5}}{n_{J'_i=1}} = \frac{\left[ 2I^\perp + I^\parallel \right]_{\text{Probe } J_i=5 \rightarrow G^1 \Pi_g}}{\left[ 2I^\perp + I^\parallel \right]_{\text{Probe } J'_i=1 \rightarrow G^1 \Pi_g}}, \quad (\text{D15})$$

and

$$\frac{n_{J_i=7}}{n_{J'_i=1}} = \frac{\left[ 2I^\perp + I^\parallel \right]_{\text{Probe } J_i=7 \rightarrow G^1 \Pi_g}}{\left[ 2I^\perp + I^\parallel \right]_{\text{Probe } J'_i=1 \rightarrow G^1 \Pi_g}}. \quad (\text{D16})$$

Thus, Eqs. (D11)-(D13) become

$$R_{J_i=3} = \frac{\left[2I^\perp + I^\parallel\right]_{\text{Probe } J_i=3 \rightarrow G^1\Pi_g}}{\left[2I^\perp + I^\parallel\right]_{\text{Probe } J'_i=1 \rightarrow G^1\Pi_g}} = \left[ \frac{165Q^2 z_{13} + 105Qz_{13}z_{15} + 77Qz_{15}z_{17} - 121z_{13}^3 + 77z_{13}^2 z_{17} + 77z_{13}z_{15}^2}{165Q^3 - 226Qz_{13}^2 - 77Qz_{15}^2 - 154z_{13}^2 z_{15}} \right], \quad (\text{D17})$$

$$R_{J_i=5} = \frac{\left[2I^\perp + I^\parallel\right]_{\text{Probe } J_i=5 \rightarrow G^1\Pi_g}}{\left[2I^\perp + I^\parallel\right]_{\text{Probe } J'_i=1 \rightarrow G^1\Pi_g}} = \left[ \frac{165Q^2 z_{15} + 165Qz_{13}^2 + 121Qz_{13}z_{17} + 121z_{13}^2 z_{15} + 77z_{13}z_{15}z_{17} - 77z_{15}^3}{165Q^3 - 226Qz_{13}^2 - 77Qz_{15}^2 - 154z_{13}^2 z_{15}} \right], \quad (\text{D18})$$

and

$$R_{J_i=7} = \frac{\left[2I^\perp + I^\parallel\right]_{\text{Probe } J_i=7 \rightarrow G^1\Pi_g}}{\left[2I^\perp + I^\parallel\right]_{\text{Probe } J'_i=1 \rightarrow G^1\Pi_g}} = \left[ \frac{165Q^2 z_{17} + 330Qz_{13}z_{15} + 165z_{13}^3 - 105z_{13}^2 z_{17} + 105z_{13}z_{15}^2}{165Q^3 - 226Qz_{13}^2 - 77Qz_{15}^2 - 154z_{13}^2 z_{15}} \right]. \quad (\text{D19})$$

Eqs. (D17)-(D19) [(31)-(33) of the main text] for the  $J$ -changing data obtained using  $G^1\Pi_g (v_e = 5, J_e = J_i) \leftarrow A^1\Sigma_u^+ (v_i = 5, J_i = 3, 5, 7)$  and  $G^1\Pi_g (v_e = 5, J'_e = J'_i) \leftarrow A^1\Sigma_u^+ (v_i = 5, J'_i = 1)$  probe transitions, along with Eqs. (22) and (23) of the main text for the  $M$ -changing data obtained using  $G^1\Pi_g (v_e = 5, J_e = J_i = 1) \leftarrow A^1\Sigma_u^+ (v_i = 5, J_i = 1)$  and  $M$ -changing data obtained using  $F^1\Sigma_g^+ (v_e = 12, J_e = 0) \leftarrow A^1\Sigma_u^+ (v_i = 5, J_i = 1)$  probe transitions, respectively, served as the fitting functions in the analysis that includes multiple collision corrections.

## Appendix E – Error bars for use in the analysis that includes multiple collision corrections

Uncertainties in the dependent variable [left hand sides of Eqs. (22), (23), (31), (32), and (33) of the main text] due to uncertainties in the intensity measurements are given by Eqs. (B8), (B12), and (B19). Again, we incorporate the effects of the uncertainty in the noble gas density into the overall uncertainty in the dependent variable using the same methods employed in

Appendix B. The calculation of  $\left. \frac{dR_{J_i=1}}{dn_{NG}} \right|_{\Delta n_{NG}}$  in Eq. (B20) remains unchanged, so that the

overall error bars associated with the  $M$ -changing data obtained using  $G^1\Pi_g (v_e = 5, J_e = J_i = 1) \leftarrow A^1\Sigma_u^+ (v_i = 5, J_i = 1)$  probe transitions and  $M$ -changing data obtained using  $F^1\Sigma_g^+ (v_e = 12, J_e = 0) \leftarrow A^1\Sigma_u^+ (v_i = 5, J_i = 1)$  probe transitions, respectively [Eqs. (26) and (27) of the main text], remain the same as in the single collision analysis. However, the form of the right hand sides of Eqs. (D17)-(D19) [Eqs. (31)-(33) of the main text] are much more

complicated than the right hand side of Eq. (24), so the derivatives  $\left. \frac{dR_{J_i=3,5,7}}{dn_{NG}} \right| \Delta n_{NG}$  are also more complicated. Nevertheless, they are straightforward to calculate, and we find

$$\left. \frac{dR_{J_i=3}}{dn_{NG}} \right| \Delta n_{NG} = \frac{\left( \begin{aligned} &330\tilde{k}_{NG}^Q Qz_{13} + 165\tilde{k}_{NG}^{J'_i=1 \rightarrow J_i=3} Q^2 + 105\tilde{k}_{NG}^Q z_{13}z_{15} + 105\tilde{k}_{NG}^{J'_i=1 \rightarrow J_i=3} Qz_{15} + 105\tilde{k}_{NG}^{J'_i=1 \rightarrow J_i=5} Qz_{13} \\ &+ 77\tilde{k}_{NG}^Q z_{15}z_{17} + 77\tilde{k}_{NG}^{J'_i=1 \rightarrow J_i=5} Qz_{17} + 77\tilde{k}_{NG}^{J'_i=1 \rightarrow J_i=7} Qz_{15} - 363\tilde{k}_{NG}^{J'_i=1 \rightarrow J_i=3} z_{13}^2 \\ &+ 154\tilde{k}_{NG}^{J'_i=1 \rightarrow J_i=3} z_{13}z_{17} + 77\tilde{k}_{NG}^{J'_i=1 \rightarrow J_i=7} z_{13}^2 + 77\tilde{k}_{NG}^{J'_i=1 \rightarrow J_i=3} z_{15}^2 + 154\tilde{k}_{NG}^{J'_i=1 \rightarrow J_i=5} z_{13}z_{15} \end{aligned} \right) - R_{J_i=3} \left( \begin{aligned} &495\tilde{k}_{NG}^Q Q^2 - 226\tilde{k}_{NG}^Q z_{13}^2 - 452\tilde{k}_{NG}^{J'_i=1 \rightarrow J_i=3} Qz_{13} - 77\tilde{k}_{NG}^Q z_{15}^2 - 154\tilde{k}_{NG}^{J'_i=1 \rightarrow J_i=5} Qz_{15} \\ &- 308\tilde{k}_{NG}^{J'_i=1 \rightarrow J_i=3} z_{13}z_{15} - 154\tilde{k}_{NG}^{J'_i=1 \rightarrow J_i=5} z_{13}^2 \end{aligned} \right)}{165Q^3 - 226Qz_{13}^2 - 77Qz_{15}^2 - 154z_{13}^2z_{15}} \Delta n_{NG}, \quad (\text{E1})$$

$$\left. \frac{dR_{J_i=5}}{dn_{NG}} \right| \Delta n_{NG} = \frac{\left( \begin{aligned} &330\tilde{k}_{NG}^Q Qz_{15} + 165\tilde{k}_{NG}^{J'_i=1 \rightarrow J_i=5} Q^2 + 165\tilde{k}_{NG}^Q z_{13}^2 + 330\tilde{k}_{NG}^{J'_i=1 \rightarrow J_i=3} Qz_{13} + 121\tilde{k}_{NG}^Q z_{13}z_{17} \\ &+ 121\tilde{k}_{NG}^{J'_i=1 \rightarrow J_i=3} Qz_{17} + 121\tilde{k}_{NG}^{J'_i=1 \rightarrow J_i=7} Qz_{13} + 242\tilde{k}_{NG}^{J'_i=1 \rightarrow J_i=3} z_{13}z_{15} + 121\tilde{k}_{NG}^{J'_i=1 \rightarrow J_i=5} z_{13}^2 \\ &+ 77\tilde{k}_{NG}^{J'_i=1 \rightarrow J_i=3} z_{15}z_{17} + 77\tilde{k}_{NG}^{J'_i=1 \rightarrow J_i=5} z_{13}z_{17} + 77\tilde{k}_{NG}^{J'_i=1 \rightarrow J_i=7} z_{13}z_{15} - 231\tilde{k}_{NG}^{J'_i=1 \rightarrow J_i=5} z_{15}^2 \end{aligned} \right) - R_{J_i=5} \left( \begin{aligned} &495\tilde{k}_{NG}^Q Q^2 - 226\tilde{k}_{NG}^Q z_{13}^2 - 452\tilde{k}_{NG}^{J'_i=1 \rightarrow J_i=3} Qz_{13} - 77\tilde{k}_{NG}^Q z_{15}^2 \\ &- 154\tilde{k}_{NG}^{J'_i=1 \rightarrow J_i=5} Qz_{15} - 308\tilde{k}_{NG}^{J'_i=1 \rightarrow J_i=3} z_{13}z_{15} - 154\tilde{k}_{NG}^{J'_i=1 \rightarrow J_i=5} z_{13}^2 \end{aligned} \right)}{165Q^3 - 226Qz_{13}^2 - 77Qz_{15}^2 - 154z_{13}^2z_{15}} \Delta n_{NG}, \quad (\text{E2})$$

and

$$\left. \frac{dR_{J_i=7}}{dn_{NG}} \right| \Delta n_{NG} = \frac{\left( \begin{aligned} &330\tilde{k}_{NG}^Q Qz_{17} + 165\tilde{k}_{NG}^{J'_i=1 \rightarrow J_i=7} Q^2 + 330\tilde{k}_{NG}^Q z_{13}z_{15} + 330\tilde{k}_{NG}^{J'_i=1 \rightarrow J_i=3} Qz_{15} \\ &+ 330\tilde{k}_{NG}^{J'_i=1 \rightarrow J_i=5} Qz_{13} + 495\tilde{k}_{NG}^{J'_i=1 \rightarrow J_i=3} z_{13}^2 - 210\tilde{k}_{NG}^{J'_i=1 \rightarrow J_i=3} z_{13}z_{17} - 105\tilde{k}_{NG}^{J'_i=1 \rightarrow J_i=7} z_{13}^2 \\ &+ 105\tilde{k}_{NG}^{J'_i=1 \rightarrow J_i=3} z_{15}^2 + 210\tilde{k}_{NG}^{J'_i=1 \rightarrow J_i=5} z_{13}z_{15} \end{aligned} \right)}{-R_{J_i=7} \left( \begin{aligned} &495\tilde{k}_{NG}^Q Q^2 - 226\tilde{k}_{NG}^Q z_{13}^2 - 452\tilde{k}_{NG}^{J'_i=1 \rightarrow J_i=3} Qz_{13} - 77\tilde{k}_{NG}^Q z_{15}^2 \\ &- 154\tilde{k}_{NG}^{J'_i=1 \rightarrow J_i=5} Qz_{15} - 308\tilde{k}_{NG}^{J'_i=1 \rightarrow J_i=3} z_{13}z_{15} - 154\tilde{k}_{NG}^{J'_i=1 \rightarrow J_i=5} z_{13}^2 \end{aligned} \right)} \Delta n_{NG}.$$

(E3)

These results are combined with Eqs. (26), (27), and (B19) to provide overall error bars for the various types of data:

$$\Delta R_{J_i=1(G^1\Pi_g)} = \left| \frac{\tilde{k}_{NG}^{J_i=1, M_i=0 \rightarrow \pm 1}}{\left( \tilde{k}_{NG}^{J_i=1, M_i=0 \rightarrow \pm 1} n_{NG} + C_1 \right)} - \frac{\tilde{k}_{NG}^Q}{\left( 1 + \tilde{k}_{NG}^Q n_{NG} + C_Q \right)} \right| \left( \frac{\tilde{k}_{NG}^{J_i=1, M_i=0 \rightarrow \pm 1} n_{NG} + C_1}{1 + \tilde{k}_{NG}^Q n_{NG} + C_Q} \right) \Delta n_{NG}$$

(E4)

$$+ 6 \left| \frac{I^\perp + I^\parallel}{\left( 2I^\perp - I^\parallel \right)^2} \right|_{\text{Probe } J_i=1 \rightarrow G^1\Pi_g} (\Delta I),$$

$$\Delta R_{J_i=1(F^1\Sigma_g^+)} = \left| \frac{\tilde{k}_{NG}^{J_i=1, M_i=0 \rightarrow \pm 1}}{\left( \tilde{k}_{NG}^{J_i=1, M_i=0 \rightarrow \pm 1} n_{NG} + C_1 \right)} - \frac{\tilde{k}_{NG}^Q}{\left( 1 + \tilde{k}_{NG}^Q n_{NG} + C_Q \right)} \right| \left( \frac{\tilde{k}_{NG}^{J_i=1, M_i=0 \rightarrow \pm 1} n_{NG} + C_1}{1 + \tilde{k}_{NG}^Q n_{NG} + C_Q} \right) \Delta n_{NG}$$

(E5)

$$+ 3 \left| \frac{I^\perp + I^\parallel}{\left( I^\parallel \right)^2} \right|_{\text{Probe } J_i=1 \rightarrow F^1\Sigma_g^+} (\Delta I),$$

$$\begin{aligned}
\Delta R_{J_i=3} = & \left( \begin{aligned} & 330\tilde{k}_{NG}^Q Qz_{13} + 165\tilde{k}_{NG}^{J'_i=1 \rightarrow J_i=3} Q^2 + 105\tilde{k}_{NG}^Q z_{13}z_{15} + 105\tilde{k}_{NG}^{J'_i=1 \rightarrow J_i=3} Qz_{15} + 105\tilde{k}_{NG}^{J'_i=1 \rightarrow J_i=5} Qz_{13} \\ & + 77\tilde{k}_{NG}^Q z_{15}z_{17} + 77\tilde{k}_{NG}^{J'_i=1 \rightarrow J_i=5} Qz_{17} + 77\tilde{k}_{NG}^{J'_i=1 \rightarrow J_i=7} Qz_{15} - 363\tilde{k}_{NG}^{J'_i=1 \rightarrow J_i=3} z_{13}^2 \\ & + 154\tilde{k}_{NG}^{J'_i=1 \rightarrow J_i=3} z_{13}z_{17} + 77\tilde{k}_{NG}^{J'_i=1 \rightarrow J_i=7} z_{13}^2 + 77\tilde{k}_{NG}^{J'_i=1 \rightarrow J_i=3} z_{15}^2 + 154\tilde{k}_{NG}^{J'_i=1 \rightarrow J_i=5} z_{13}z_{15} \end{aligned} \right) \\
& - R_{J_i=3} \left( \begin{aligned} & 495\tilde{k}_{NG}^Q Q^2 - 226\tilde{k}_{NG}^Q z_{13}^2 - 452\tilde{k}_{NG}^{J'_i=1 \rightarrow J_i=3} Qz_{13} - 77\tilde{k}_{NG}^Q z_{15}^2 \\ & - 154\tilde{k}_{NG}^{J'_i=1 \rightarrow J_i=5} Qz_{15} - 308\tilde{k}_{NG}^{J'_i=1 \rightarrow J_i=3} z_{13}z_{15} - 154\tilde{k}_{NG}^{J'_i=1 \rightarrow J_i=5} z_{13}^2 \end{aligned} \right) \\
& \frac{\Delta n_{NG}}{165Q^3 - 226Qz_{13}^2 - 77Qz_{15}^2 - 154z_{13}^2z_{15}} \\
& + 9 \left| \frac{\left[ 2I^\perp + I^\parallel \right]_{\text{Probe } J_i=3 \rightarrow G^1\Pi_g} + \left[ 2I^\perp + I^\parallel \right]_{\text{Probe } J'_i=1 \rightarrow G^1\Pi_g}}{\left[ 2I^\perp + I^\parallel \right]_{\text{Probe } J'_i=1 \rightarrow G^1\Pi_g}^2} (\Delta I), \right. \\
& \left. \right. \tag{E6}
\end{aligned}$$

$$\begin{aligned}
\Delta R_{J_i=5} = & \left( \begin{aligned} & 330\tilde{k}_{NG}^Q Qz_{15} + 165\tilde{k}_{NG}^{J'_i=1 \rightarrow J_i=5} Q^2 + 165\tilde{k}_{NG}^Q z_{13}^2 + 330\tilde{k}_{NG}^{J'_i=1 \rightarrow J_i=3} Qz_{13} + 121\tilde{k}_{NG}^Q z_{13}z_{17} \\ & + 121\tilde{k}_{NG}^{J'_i=1 \rightarrow J_i=3} Qz_{17} + 121\tilde{k}_{NG}^{J'_i=1 \rightarrow J_i=7} Qz_{13} + 242\tilde{k}_{NG}^{J'_i=1 \rightarrow J_i=3} z_{13}z_{15} + 121\tilde{k}_{NG}^{J'_i=1 \rightarrow J_i=5} z_{13}^2 \\ & + 77\tilde{k}_{NG}^{J'_i=1 \rightarrow J_i=3} z_{15}z_{17} + 77\tilde{k}_{NG}^{J'_i=1 \rightarrow J_i=5} z_{13}z_{17} + 77\tilde{k}_{NG}^{J'_i=1 \rightarrow J_i=7} z_{13}z_{15} - 231\tilde{k}_{NG}^{J'_i=1 \rightarrow J_i=5} z_{15}^2 \end{aligned} \right) \\
& - R_{J_i=5} \left( \begin{aligned} & 495\tilde{k}_{NG}^Q Q^2 - 226\tilde{k}_{NG}^Q z_{13}^2 - 452\tilde{k}_{NG}^{J'_i=1 \rightarrow J_i=3} Qz_{13} - 77\tilde{k}_{NG}^Q z_{15}^2 \\ & - 154\tilde{k}_{NG}^{J'_i=1 \rightarrow J_i=5} Qz_{15} - 308\tilde{k}_{NG}^{J'_i=1 \rightarrow J_i=3} z_{13}z_{15} - 154\tilde{k}_{NG}^{J'_i=1 \rightarrow J_i=5} z_{13}^2 \end{aligned} \right) \\
& \frac{\Delta n_{NG}}{165Q^3 - 226Qz_{13}^2 - 77Qz_{15}^2 - 154z_{13}^2z_{15}} \\
& + 9 \left| \frac{\left[ 2I^\perp + I^\parallel \right]_{\text{Probe } J_i=5 \rightarrow G^1\Pi_g} + \left[ 2I^\perp + I^\parallel \right]_{\text{Probe } J'_i=1 \rightarrow G^1\Pi_g}}{\left[ 2I^\perp + I^\parallel \right]_{\text{Probe } J'_i=1 \rightarrow G^1\Pi_g}^2} (\Delta I), \right. \\
& \left. \right. \tag{E7}
\end{aligned}$$

and

$$\begin{aligned}
\Delta R_{J_i=7} = & \frac{\left( \begin{aligned} & 330\tilde{k}_{NG}^Q Q z_{17} + 165\tilde{k}_{NG}^{J'_i=1 \rightarrow J_i=7} Q^2 + 330\tilde{k}_{NG}^Q z_{13} z_{15} + 330\tilde{k}_{NG}^{J'_i=1 \rightarrow J_i=3} Q z_{15} \\ & + 330\tilde{k}_{NG}^{J'_i=1 \rightarrow J_i=5} Q z_{13} + 495\tilde{k}_{NG}^{J'_i=1 \rightarrow J_i=3} z_{13}^2 - 210\tilde{k}_{NG}^{J'_i=1 \rightarrow J_i=3} z_{13} z_{17} - 105\tilde{k}_{NG}^{J'_i=1 \rightarrow J_i=7} z_{13}^2 \\ & + 105\tilde{k}_{NG}^{J'_i=1 \rightarrow J_i=3} z_{15}^2 + 210\tilde{k}_{NG}^{J'_i=1 \rightarrow J_i=5} z_{13} z_{15} \end{aligned} \right)}{165Q^3 - 226Qz_{13}^2 - 77Qz_{15}^2 - 154z_{13}^2 z_{15}} \Delta n_{NG} \\
& + 9 \left| \frac{\left[ 2I^\perp + I^\parallel \right]_{\text{Probe } J_i=7 \rightarrow G^1 \Pi_g} + \left[ 2I^\perp + I^\parallel \right]_{\text{Probe } J'_i=1 \rightarrow G^1 \Pi_g}}{\left[ 2I^\perp + I^\parallel \right]_{\text{Probe } J'_i=1 \rightarrow G^1 \Pi_g}^2} \right| (\Delta I).
\end{aligned} \tag{E8}$$

Note that in Eqs. (E1), (E2), and (E3), and also in Eqs. (E6), (E7), and (E8), one should use expressions for  $R_{J_i=3}$ ,  $R_{J_i=5}$ , and  $R_{J_i=7}$  in terms of the rate coefficients as written on the right hand sides of Eqs. (D17), (D18), and (D19) [Eqs. (31), (32), and (33) of the main text], respectively.

## Appendix F – Single collision model fits in which high pressure data points for inelastic collisions were excluded

We carried out a series of fits, using the single collision approximation, Eqs. (22), (23), and (24) for the  $M$ -changing data obtained using the  $G^1\Pi_g(v_e = 5, J_e = J_i = 1) \leftarrow A^1\Sigma_u^+(v_i = 5, J_i = 1)$  probe transition,  $M$ -changing data obtained using the  $F^1\Sigma_g^+(v_e = 12, J_e = 0) \leftarrow A^1\Sigma_u^+(v_i = 5, J_i = 1)$  probe transition, and  $J$ -changing data obtained using the  $G^1\Pi_g(v_e = 5, J_e = J_i) \leftarrow A^1\Sigma_u^+(v_i = 5, J_i = 3, 5, 7)$  and  $G^1\Pi_g(v_e = 5, J_e = J'_i) \leftarrow A^1\Sigma_u^+(v_i = 5, J'_i = 1)$  probe transitions, respectively, with weightings given in Eqs. (26), (27), and (28) [(B21), (B22), and (B24)], respectively. In these fits inelastic collision data for pressures above a chosen cutoff pressure were excluded from the corresponding fit. These high pressure inelastic collision data are most susceptible to multiple collision effects. Therefore, the validity of the single collision approximation increases as the cutoff pressure decreases. Cutoff pressures of 10, 7, 5, and 3 Torr were chosen. Results of the single collision model fits, with these cutoff pressures, are presented in Tables F.1, F.2, F.3, and F.4 below.

Table F.1 – Results of the single collision model fit with inelastic collision data corresponding to pressures above 10 Torr excluded. Rate coefficients ( $k_{Ar,He}^{J_i=1,M_i=0 \rightarrow \pm 1}$  and  $k_{Ar,He}^{J'_i=1 \rightarrow J_i=3,5,7}$ ) divided by the radiative rate  $\Gamma$  and in units of  $\text{cm}^3 \text{s}^{-1}$  [the latter obtained by multiplying the fitted parameters ( $\tilde{k}_{Ar,He}^{J_i=1,M_i=0 \rightarrow \pm 1}$  and  $\tilde{k}_{Ar,He}^{J'_i=1 \rightarrow J_i=3,5,7}$ ) by  $\Gamma = 5.45 \times 10^7 \text{ s}^{-1}$  [8]] for  $M$ -changing (elastic) collisions,  $A^1\Sigma_u^+(v_i = 5, J_i = 1, M_i = 0) \rightarrow A^1\Sigma_u^+(v_i = 5, J_i = 1, M_i = \pm 1)$ , and for  $J$ -changing (inelastic) collisions,  $A^1\Sigma_u^+(v_i = 5, J'_i = 1) \rightarrow A^1\Sigma_u^+(v_i = 5, J_i = 3, 5, 7)$ , of  $\text{Li}_2$  molecules with argon and helium atoms are reported. Quenching rate coefficients are also given. Quoted uncertainties represent statistical errors only. Systematic errors due to neglect of multiple collision effects are expected to be much larger.

$M$ -changing	$\tilde{k}_{Ar}^{J_i=1,M_i=0 \rightarrow \pm 1}$ ( $10^{-18} \text{ cm}^3$ )	$\tilde{k}_{He}^{J_i=1,M_i=0 \rightarrow \pm 1}$ ( $10^{-18} \text{ cm}^3$ )	$k_{Ar}^{J_i=1,M_i=0 \rightarrow \pm 1}$ ( $10^{-11} \text{ cm}^3 \text{ s}^{-1}$ )	$k_{He}^{J_i=1,M_i=0 \rightarrow \pm 1}$ ( $10^{-11} \text{ cm}^3 \text{ s}^{-1}$ )
$J_i = 1, M_i = 0 \rightarrow J_i = 1, M_i = \pm 1$	1.40 $\pm$ 0.06	0.99 $\pm$ 0.05	7.65 $\pm$ 0.31	5.38 $\pm$ 0.28
$J$ -changing	$\tilde{k}_{Ar}^{J'_i=1 \rightarrow J_i=3,5,7}$ ( $10^{-18} \text{ cm}^3$ )	$\tilde{k}_{He}^{J'_i=1 \rightarrow J_i=3,5,7}$ ( $10^{-18} \text{ cm}^3$ )	$k_{Ar}^{J'_i=1 \rightarrow J_i=3,5,7}$ ( $10^{-11} \text{ cm}^3 \text{ s}^{-1}$ )	$k_{He}^{J'_i=1 \rightarrow J_i=3,5,7}$ ( $10^{-11} \text{ cm}^3 \text{ s}^{-1}$ )
$J'_i = 1 \rightarrow J_i = 3$	6.97 $\pm$ 0.26	5.10 $\pm$ 0.25	38.0 $\pm$ 1.4	27.8 $\pm$ 1.4
$J'_i = 1 \rightarrow J_i = 5$	4.73 $\pm$ 0.18	4.52 $\pm$ 0.23	25.8 $\pm$ 1.0	24.7 $\pm$ 1.2
$J'_i = 1 \rightarrow J_i = 7$	3.80 $\pm$ 0.15	4.15 $\pm$ 0.21	20.7 $\pm$ 0.8	22.6 $\pm$ 1.1
Quenching	$\tilde{k}_{Ar}^Q$ ( $10^{-18} \text{ cm}^3$ )	$\tilde{k}_{He}^Q$ ( $10^{-18} \text{ cm}^3$ )	$k_{Ar}^Q$ ( $10^{-11} \text{ cm}^3 \text{ s}^{-1}$ )	$k_{He}^Q$ ( $10^{-11} \text{ cm}^3 \text{ s}^{-1}$ )
	13.7 $\pm$ 0.8	15.0 $\pm$ 1.2	74.8 $\pm$ 4.6	82.0 $\pm$ 6.7

Table F.2 – Results of the single collision model fit with inelastic collision data corresponding to pressures above 7 Torr excluded. Rate coefficients ( $k_{Ar,He}^{J_i=1,M_i=0 \rightarrow \pm 1}$  and  $k_{Ar,He}^{J'_i=1 \rightarrow J_i=3,5,7}$ ) divided by the radiative rate  $\Gamma$  and in units of  $\text{cm}^3\text{s}^{-1}$  [the latter obtained by multiplying the fitted parameters ( $\tilde{k}_{Ar,He}^{J_i=1,M_i=0 \rightarrow \pm 1}$  and  $\tilde{k}_{Ar,He}^{J'_i=1 \rightarrow J_i=3,5,7}$ ) by  $\Gamma = 5.45 \times 10^7 \text{ s}^{-1}$  [8]] for  $M$ -changing (elastic) collisions,  $A^1\Sigma_u^+(v_i=5, J_i=1, M_i=0) \rightarrow A^1\Sigma_u^+(v_i=5, J_i=1, M_i=\pm 1)$ , and for  $J$ -changing (inelastic) collisions,  $A^1\Sigma_u^+(v_i=5, J'_i=1) \rightarrow A^1\Sigma_u^+(v_i=5, J_i=3,5,7)$ , of  $\text{Li}_2$  molecules with argon and helium atoms are reported. Quenching rate coefficients are also given. Quoted uncertainties represent statistical errors only. Systematic errors due to neglect of multiple collision effects are expected to be much larger.

$M$ -changing	$\tilde{k}_{Ar}^{J_i=1,M_i=0 \rightarrow \pm 1}$ ( $10^{-18} \text{ cm}^3$ )	$\tilde{k}_{He}^{J_i=1,M_i=0 \rightarrow \pm 1}$ ( $10^{-18} \text{ cm}^3$ )	$k_{Ar}^{J_i=1,M_i=0 \rightarrow \pm 1}$ ( $10^{-11} \text{ cm}^3\text{s}^{-1}$ )	$k_{He}^{J_i=1,M_i=0 \rightarrow \pm 1}$ ( $10^{-11} \text{ cm}^3\text{s}^{-1}$ )	
	$J_i=1, M_i=0 \rightarrow J_i=1, M_i=\pm 1$	1.53 $\pm$ 0.06	1.09 $\pm$ 0.06	8.35 $\pm$ 0.33	5.96 $\pm$ 0.32
$J$ -changing	$\tilde{k}_{Ar}^{J'_i=1 \rightarrow J_i=3,5,7}$ ( $10^{-18} \text{ cm}^3$ )	$\tilde{k}_{He}^{J'_i=1 \rightarrow J_i=3,5,7}$ ( $10^{-18} \text{ cm}^3$ )	$k_{Ar}^{J'_i=1 \rightarrow J_i=3,5,7}$ ( $10^{-11} \text{ cm}^3\text{s}^{-1}$ )	$k_{He}^{J'_i=1 \rightarrow J_i=3,5,7}$ ( $10^{-11} \text{ cm}^3\text{s}^{-1}$ )	
	$J'_i=1 \rightarrow J_i=3$	7.41 $\pm$ 0.27	5.55 $\pm$ 0.26	40.4 $\pm$ 1.5	30.3 $\pm$ 1.4
	$J'_i=1 \rightarrow J_i=5$	4.78 $\pm$ 0.18	4.72 $\pm$ 0.23	26.1 $\pm$ 1.0	25.7 $\pm$ 1.2
	$J'_i=1 \rightarrow J_i=7$	3.59 $\pm$ 0.14	4.14 $\pm$ 0.20	19.6 $\pm$ 0.8	22.6 $\pm$ 1.1
Quenching	$\tilde{k}_{Ar}^Q$ ( $10^{-18} \text{ cm}^3$ )	$\tilde{k}_{He}^Q$ ( $10^{-18} \text{ cm}^3$ )	$k_{Ar}^Q$ ( $10^{-11} \text{ cm}^3\text{s}^{-1}$ )	$k_{He}^Q$ ( $10^{-11} \text{ cm}^3\text{s}^{-1}$ )	
	15.6 $\pm$ 0.9	17.7 $\pm$ 1.4	85.1 $\pm$ 4.9	96.2 $\pm$ 7.5	

Table F.3 – Results of the single collision model fit with inelastic collision data corresponding to pressures above 5 Torr excluded. Rate coefficients ( $k_{Ar,He}^{J_i=1,M_i=0 \rightarrow \pm 1}$  and  $k_{Ar,He}^{J'_i=1 \rightarrow J_i=3,5,7}$ ) divided by the radiative rate  $\Gamma$  and in units of  $\text{cm}^3\text{s}^{-1}$  [the latter obtained by multiplying the fitted parameters ( $\tilde{k}_{Ar,He}^{J_i=1,M_i=0 \rightarrow \pm 1}$  and  $\tilde{k}_{Ar,He}^{J'_i=1 \rightarrow J_i=3,5,7}$ ) by  $\Gamma = 5.45 \times 10^7 \text{ s}^{-1}$  [8]] for  $M$ -changing (elastic) collisions,  $A^1\Sigma_u^+(v_i=5, J_i=1, M_i=0) \rightarrow A^1\Sigma_u^+(v_i=5, J_i=1, M_i=\pm 1)$ , and for  $J$ -changing (inelastic) collisions,  $A^1\Sigma_u^+(v_i=5, J'_i=1) \rightarrow A^1\Sigma_u^+(v_i=5, J_i=3,5,7)$ , of  $\text{Li}_2$  molecules with argon and helium atoms are reported. Quenching rate coefficients are also given. Quoted uncertainties represent statistical errors only. Systematic errors due to neglect of multiple collision effects are expected to be much larger.

$M$ -changing	$\tilde{k}_{Ar}^{J_i=1,M_i=0 \rightarrow \pm 1}$ ( $10^{-18} \text{ cm}^3$ )	$\tilde{k}_{He}^{J_i=1,M_i=0 \rightarrow \pm 1}$ ( $10^{-18} \text{ cm}^3$ )	$k_{Ar}^{J_i=1,M_i=0 \rightarrow \pm 1}$ ( $10^{-11} \text{ cm}^3\text{s}^{-1}$ )	$k_{He}^{J_i=1,M_i=0 \rightarrow \pm 1}$ ( $10^{-11} \text{ cm}^3\text{s}^{-1}$ )	
	$J_i=1, M_i=0 \rightarrow J_i=1, M_i=\pm 1$	1.59 $\pm$ 0.06	1.14 $\pm$ 0.06	8.67 $\pm$ 0.35	6.20 $\pm$ 0.35
$J$ -changing	$\tilde{k}_{Ar}^{J'_i=1 \rightarrow J_i=3,5,7}$ ( $10^{-18} \text{ cm}^3$ )	$\tilde{k}_{He}^{J'_i=1 \rightarrow J_i=3,5,7}$ ( $10^{-18} \text{ cm}^3$ )	$k_{Ar}^{J'_i=1 \rightarrow J_i=3,5,7}$ ( $10^{-11} \text{ cm}^3\text{s}^{-1}$ )	$k_{He}^{J'_i=1 \rightarrow J_i=3,5,7}$ ( $10^{-11} \text{ cm}^3\text{s}^{-1}$ )	
	$J'_i=1 \rightarrow J_i=3$	7.51 $\pm$ 0.30	5.73 $\pm$ 0.29	40.9 $\pm$ 1.6	31.3 $\pm$ 1.6
	$J'_i=1 \rightarrow J_i=5$	4.69 $\pm$ 0.20	4.74 $\pm$ 0.25	25.6 $\pm$ 1.1	25.8 $\pm$ 1.4
	$J'_i=1 \rightarrow J_i=7$	3.34 $\pm$ 0.15	3.94 $\pm$ 0.21	18.2 $\pm$ 0.8	21.5 $\pm$ 1.2
Quenching	$\tilde{k}_{Ar}^Q$ ( $10^{-18} \text{ cm}^3$ )	$\tilde{k}_{He}^Q$ ( $10^{-18} \text{ cm}^3$ )	$k_{Ar}^Q$ ( $10^{-11} \text{ cm}^3\text{s}^{-1}$ )	$k_{He}^Q$ ( $10^{-11} \text{ cm}^3\text{s}^{-1}$ )	
	16.5 $\pm$ 1.0	18.7 $\pm$ 1.5	90.0 $\pm$ 5.2	102 $\pm$ 8.4	

Table F.4 – Results of the single collision model fit with inelastic collision data corresponding to pressures above 3 Torr excluded. Rate coefficients ( $k_{Ar,He}^{J_i=1,M_i=0 \rightarrow \pm 1}$  and  $k_{Ar,He}^{J'_i=1 \rightarrow J_i=3,5,7}$ ) divided by the radiative rate  $\Gamma$  and in units of  $\text{cm}^3\text{s}^{-1}$  [the latter obtained by multiplying the fitted parameters ( $\tilde{k}_{Ar,He}^{J_i=1,M_i=0 \rightarrow \pm 1}$  and  $\tilde{k}_{Ar,He}^{J'_i=1 \rightarrow J_i=3,5,7}$ ) by  $\Gamma = 5.45 \times 10^7 \text{ s}^{-1}$  [8]] for  $M$ -changing (elastic) collisions,  $A^1\Sigma_u^+(v_i=5, J_i=1, M_i=0) \rightarrow A^1\Sigma_u^+(v_i=5, J_i=1, M_i=\pm 1)$ , and for  $J$ -changing (inelastic) collisions,  $A^1\Sigma_u^+(v_i=5, J'_i=1) \rightarrow A^1\Sigma_u^+(v_i=5, J_i=3,5,7)$ , of  $\text{Li}_2$  molecules with argon and helium atoms are reported. Quenching rate coefficients are also given. Quoted uncertainties represent statistical errors only. Systematic errors due to neglect of multiple collision effects are expected to be much larger.

$M$ -changing	$\tilde{k}_{Ar}^{J_i=1,M_i=0 \rightarrow \pm 1}$ ( $10^{-18} \text{ cm}^3$ )	$\tilde{k}_{He}^{J_i=1,M_i=0 \rightarrow \pm 1}$ ( $10^{-18} \text{ cm}^3$ )	$k_{Ar}^{J_i=1,M_i=0 \rightarrow \pm 1}$ ( $10^{-11} \text{ cm}^3\text{s}^{-1}$ )	$k_{He}^{J_i=1,M_i=0 \rightarrow \pm 1}$ ( $10^{-11} \text{ cm}^3\text{s}^{-1}$ )	
	$J_i=1, M_i=0 \rightarrow J_i=1, M_i=\pm 1$	1.61 $\pm$ 0.06	1.20 $\pm$ 0.07	8.76 $\pm$ 0.35	6.53 $\pm$ 0.38
$J$ -changing	$\tilde{k}_{Ar}^{J'_i=1 \rightarrow J_i=3,5,7}$ ( $10^{-18} \text{ cm}^3$ )	$\tilde{k}_{He}^{J'_i=1 \rightarrow J_i=3,5,7}$ ( $10^{-18} \text{ cm}^3$ )	$k_{Ar}^{J'_i=1 \rightarrow J_i=3,5,7}$ ( $10^{-11} \text{ cm}^3\text{s}^{-1}$ )	$k_{He}^{J'_i=1 \rightarrow J_i=3,5,7}$ ( $10^{-11} \text{ cm}^3\text{s}^{-1}$ )	
	$J'_i=1 \rightarrow J_i=3$	7.70 $\pm$ 0.50	5.91 $\pm$ 0.41	42.0 $\pm$ 2.7	32.2 $\pm$ 2.2
	$J'_i=1 \rightarrow J_i=5$	4.49 $\pm$ 0.32	4.59 $\pm$ 0.33	24.5 $\pm$ 1.7	25.0 $\pm$ 1.8
	$J'_i=1 \rightarrow J_i=7$	2.91 $\pm$ 0.22	3.48 $\pm$ 0.27	15.9 $\pm$ 1.2	19.0 $\pm$ 1.5
Quenching	$\tilde{k}_{Ar}^Q$ ( $10^{-18} \text{ cm}^3$ )	$\tilde{k}_{He}^Q$ ( $10^{-18} \text{ cm}^3$ )	$k_{Ar}^Q$ ( $10^{-11} \text{ cm}^3\text{s}^{-1}$ )	$k_{He}^Q$ ( $10^{-11} \text{ cm}^3\text{s}^{-1}$ )	
	16.8 $\pm$ 1.0	20.2 $\pm$ 1.7	91.4 $\pm$ 5.3	110 $\pm$ 9.3	

## References

1. J. Jones, K. Richter, T. J. Price, A. J. Ross, P. Crozet, C. Faust, R. F. Malenda, S. Carlus, A. P. Hickman, and J. Huennekens, *Journal of Chemical Physics* **147**, 144303 (2017).
2. G. Herzberg, *Molecular Spectra and Molecular Structure I. Spectra of Diatomic Molecules* (Van Nostrand Reinhold, New York, 1950).
3. P. F. Bernath, *Spectra of Atoms and Molecules* (Oxford University Press, New York, 1995).
4. A. Corney, *Atomic and Laser Spectroscopy* (Clarendon Press, Oxford, 1977).
5. E. U. Condon and G. H. Shortley, *The Theory of Atomic Spectra* (Cambridge University Press, Cambridge, 1991).
6. I. Kovács, *Rotational Structure in the Spectra of Diatomic Molecules* (American Elsevier, New York, 1969).
7. T. J. Price, PhD dissertation, Lehigh University, 2017.
8. A. Sanli, X. Pan, D. S. Beecher, S. Magnier, A. M. Lyyra, and a. E. H. Ahmed, *Journal of Molecular Spectroscopy* **355**, 1 (2019).